Journal of Medicinal Chemistry

pubs.acs.org/jmc

Article

Diamino Allose Phosphates: Novel, Potent, and Highly Stable Toll-like Receptor 4 Agonists

Juhienah K. Khalaf,* Laura S. Bess, Lois M. Walsh, Janine M. Ward, Craig L. Johnson, Mark T. Livesay, Konner J. Jackson, Jay T. Evans, Kendal T. Ryter, and Hélène G. Bazin-Lee

Cite This: *J. Med. Chem.* 2023, 66, 13900−13917

Read Online

ACCESS | Metrics & More | Article Recommendations | Supporting Information

ABSTRACT: Most known synthetic toll-like receptor 4 (TLR4) agonists are carbohydrate-based lipid-A mimetics containing several fatty acyl chains, including a labile 3-*O*-acyl chain linked to the C-3 position of the non-reducing sugar known to undergo cleavage impacting stability and resulting in loss of activity. To overcome this inherent instability, we rationally designed a new class of chemically more stable synthetic TLR4 ligands that elicit robust innate and adaptive immune responses. This new class utilized a diamino allose phosphate (DAP) scaffold containing a nonhydrolyzable 3-amide bond instead of the classical 3-ester. Accordingly, the DAPs have significantly improved thermostability in aqueous formulations and potency relative to other known natural and synthetic TLR4 ligands. Furthermore, the DAP analogues function as potent vaccine adjuvants to enhance influenza-specific antibodies in mice and provide protection against lethal influenza virus challenges. This novel set of TLR4 ligands show promise as next-generation vaccine adjuvants and stand-alone immunomodulators.

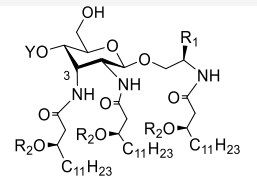

DAP Monosaccharide TLR4 agonists

8a R_1 = H, R_2 = *n*-$C_9H_{19}CO$, Y = $PO(OH)_2$
8b R_1 = H, R_2 = *n*-$C_9H_{19}CO$, Y = SO_3H
8c R_1 = H, R_2 = *n*-$C_9H_{19}CO$, Y = $CH_2PO(OH)_2$
17a R_1 = CO_2H, R_2 = *n*-$C_{10}H_{21}$, Y = $PO(OH)_2$
17b R_1 = CO_2H, R_2 = *n*-$C_{10}H_{21}$, Y = SO_3H
17c R_1 = CO_2H, R_2 = *n*-$C_{10}H_{21}$, Y = $CH_2PO(OH)_2$

INTRODUCTION

The rise of newly emerging and re-emerging infectious diseases in the last couple of decades has prompted an upsurge in the development of vaccines to prevent, combat, and provide global health protection against infectious pathogens.[1−3] In addition to preventing infections, vaccines are also being developed to treat cancer, addiction, asthma, and autoimmune diseases.[4−6] The effectiveness of vaccines can be further enhanced using adjuvants, which contribute to directing the type and magnitude of immune responses. Upon infection, adjuvants trigger an initial innate immune response, limiting the early spread of infection by reducing the pathogen burden to tolerable levels and subsequently mediating events promoting the development of acquired immune responses to eliminate all residual traces of infection. Accordingly, adjuvants are critical components of both subunit vaccines and certain inactivated vaccines, improving both adaptive immune breadth and durability.[7−10] The clinical and commercial success of adjuvants also lies in their distinctive physicochemical properties, which can be optimized to enable long-term thermostable storage with minimum to no degradation and ease of formulation leading to vaccines being readily available for distribution and administration when new threats occur.

Notwithstanding the large number of adjuvants developed thus far, only a few are in licensed vaccines, including aluminum salts, emulsions, and toll-like receptor (TLR) agonists.[7,9,11,12] While these approved adjuvants have acceptable safety profiles and are considered effective in inducing humoral and cell-mediated immunity, there remains a continued unmet need to expand the repertoire of adjuvants available to combat new pathogen threats and improve the safety and efficacy conferred by existing vaccines. Additional challenges remain around vaccine manufacturing, storage, and stability; thus, improvements are required to increase their thermal stability in pharmaceutical formulations.

Innate immunity has evolved as the front-line defense against invading pathogens and acts through highly conserved pattern-recognition receptors (PRRs) to coordinate the innate inflammatory response to both endogenous and exogenous stimuli and further shape adaptive immunity.[13] Among the five major families of PRRs, TLRs are best characterized and broadly expressed on innate immune cells that recognize pathogen-specific components of microbial invaders. Within minutes of recognizing pathogen-associated molecular patterns (PAMPs), TLR activation triggers the induction of cytokines and costimulatory molecules, leading to the recruitment of cellular mediators critical for initiating innate immunity and the establishment of adaptive immunity. The high specificity and downstream effects of TLR activation make these receptors an attractive therapeutic target for vaccine adjuvants and immunotherapy.[14,15]

Received: April 24, 2023
Published: October 17, 2023

Downloaded via UNIV OF MONTANA on March 13, 2024 at 16:34:52 (UTC).
See https://pubs.acs.org/sharingguidelines for options on how to legitimately share published articles.

ACS Publications

© 2023 American Chemical Society

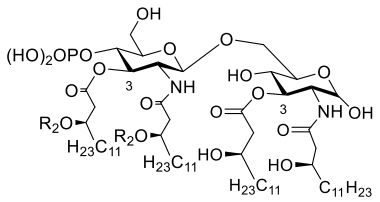

Synthetic Disaccharide TLR4 Agonist

GLA R_2= *n*-$C_{13}H_{25}CO$

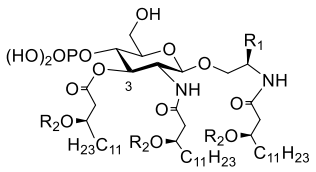

Synthetic Monosaccharide TLR4 Agonists

1a R_1 = H, R_2= *n*-$C_9H_{19}CO$

1b R_1 = CO_2H, R_2= *n*-$C_9H_{19}CO$

1c R_1 = CO_2H, R_2= *n*-$C_{10}H_{21}$

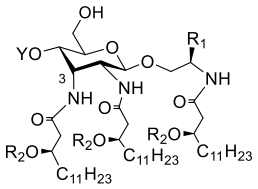

DAP Monosaccharide TLR4 agonists

8a R_1 = H, R_2 = *n*-$C_9H_{19}CO$, Y = $PO(OH)_2$

8b R_1 = H, R_2 = *n*-$C_9H_{19}CO$, Y = SO_3H

8c R_1 = H, R_2 = *n*-$C_9H_{19}CO$, Y = $CH_2PO(OH)_2$

17a R_1 = CO_2H, R_2 = *n*-$C_{10}H_{21}$, Y = $PO(OH)_2$

17b R_1 = CO_2H, R_2 = *n*-$C_{10}H_{21}$, Y = SO_3H

17c R_1 = CO_2H, R_2 = *n*-$C_{10}H_{21}$, Y = $CH_2PO(OH)_2$

Figure 1. Structures of known synthetic TLR4 agonists GLA and **1a−c** and new DAP monosaccharide TLR4 agonists **8a−c** and **17a−c**.

Among the ten different known human TLRs,[16] TLR4 is the specific sensor of lipopolysaccharide (LPS, endotoxin), one of the molecular components of the Gram-negative bacteria outer membrane. TLR4, expressed on the plasma membrane and within the endosome of most innate immune cells, forms a stable complex with its accessory molecule myeloid differentiation factor 2 (MD-2) and recognizes LPS, resulting in an initial innate immune response.[17] Although LPS is a potent stimulator of host defense systems, the acute inflammatory response induced by LPS and its active principle component, lipid A, preclude their use as adjuvants in human vaccines.[18] Thus, considerable effort has been directed toward the development of both natural and synthetic lipid A mimetics, with simplified structures and improved safety profiles for use as vaccine adjuvants and stand-alone immunotherapeutic agents.[19−22]

In the course of our own structure−activity studies on a detoxified but complex form of lipid A known as 3-*O*-desacyl monophosphoryl lipid A (MPLA), a disaccharide TLR4 agonist, we developed a new class of synthetic monosaccharide TLR4-active glycolipids known as aminoalkyl glucosaminide 4-phosphates (AGPs), capable of eliciting robust innate and adaptive immune responses.[23−26] These monosaccharide compounds consist of three fatty acyl chains that are *N*- and *O*-linked to an *O*-glucosaminyl ethylamine or serine backbone (e.g., **1a−c**, Figure 1). We demonstrated that minor structural modifications to synthetic TLR4 agonists could alter signaling selectivity[27,28] (MyD88 vs TRIF bias in TLR4 agonists) and convert agonist to antagonist responses.[25] Engineered to specifically trigger an innate immune response with varying degrees of specificity, potency, and safety attributes, some of these agonists, in addition to showing promise as vaccine adjuvants,[29−33] were also capable of eliciting nonspecific protection against a wide range of infectious pathogens.[34−37] As evidence of the validity of this approach, the TLR4 agonist RC-529[24] was approved for human use in a recombinant HBV vaccine[38] and another highly active TLR4 agonist, GSK1795091[39] (agonist **1c**[25]), completed a phase I clinical trial for safety evaluation.[40]

Replacing the labile ester-linked secondary fatty acids of the synthetic AGP **1b**, known to be degraded in vivo by acyloxyacyl hydrolase (AOAH),[41] with alkyl chains in the TLR4 agonist **1c** improved the stability of this compound.[25] However, **1c** and other approved or clinically tested TLR4 agonists, such as MPLA adjuvant or glucopyranosyl lipid A (GLA), still contain labile groups such as the primary ester at the 3-position and the phosphate at the 4-position of the conserved glucosamine. Both groups are susceptible to cleavage/migration during synthesis and formulation; in particular, the deacylation of the 3-position, the migration of the 4-phosphate group to the 6-position of the glucosamine, or the byproduct formation of the 4,6-cyclic phosphate,[42] leading to decreased stability of these products (unpublished results). Presumably, the lability of these groups and of the acyloxyacyl chains led to GLA degradation in an emulsion formulation after exposure to elevated temperatures.[43] These deficiencies along with the natural heterogeneity of a few TLR4 agonists (e.g., MPLA), stimulated our interest in developing more stable and potent fully synthetic TLR4 ligands (**8a−c** and **17a−c**, Figure 1).

Our rational design toward developing a more stable synthetic TLR4 agonist started with maintaining the phosphate functionality and converting the equatorial 3-ester moiety of the conserved glucosamine scaffold to the chemically more stable 3-amide group, prompting the design of the D-(2,3)-diamino allose phosphate (DAP) monosaccharides. The carbohydrate entity in the DAP series is highly unique as the 3-position of D-allosamine (2-amino-2-deoxy-D-allose) is deoxygenated and replaced with an amino group. D-Allosamine is a "rare" sugar itself, found in natural products of bacteria, exemplified in the formation of the core component of the chitinase inhibitor allosamidin.[44] Hence, D-2,3-diamino allose (or 3-amino-3-deoxy D-allosamine) would be considered a remarkable scaffold that has hardly been reported; therefore, it is a viable addition to the "chemical space" used in medicinal chemistry, in particular the space of TLR4 agonism. Since the 1920s, a large number of diverse LPS structures have been reported, and many synthetic glycolipid TLR4 agonists have been prepared; however, none of these include D-2,3-diamino allose as the non-reducing carbohydrate component.[14,44,45]

The second modification included substituting the phosphate group with chemically more stable bioisosteres. These modifications culminated in the synthesis of a novel series of synthetic lipid A mimetics **8a−c** and **17a−c**. The novel mimetics exhibit TLR4 ligand specificity and high potency in peripheral blood mononuclear cells (PBMCs), and more importantly, these compounds have greatly improved aqueous thermostability and a prolonged shelf life. These are crucial advantages that can support a sustainable global supply of a temperature-stable aqueous or lyophilized vaccine adjuvant and reflect potential economic benefits through substantial cost savings in appropriate storage and handling. Furthermore, we disclose preliminary studies demonstrating these novel TLR4 ligands function as adjuvants, enhancing influenza-specific antibody responses in vivo. The DAP analogue **17a** has also been shown to provide nonspecific resistance to influenza challenges in mice

https://doi.org/10.1021/acs.jmedchem.3c00724
J. Med. Chem. 2023, 66, 13900−13917

Scheme 1. Synthesis of Intermediates 2a and 3a[a]

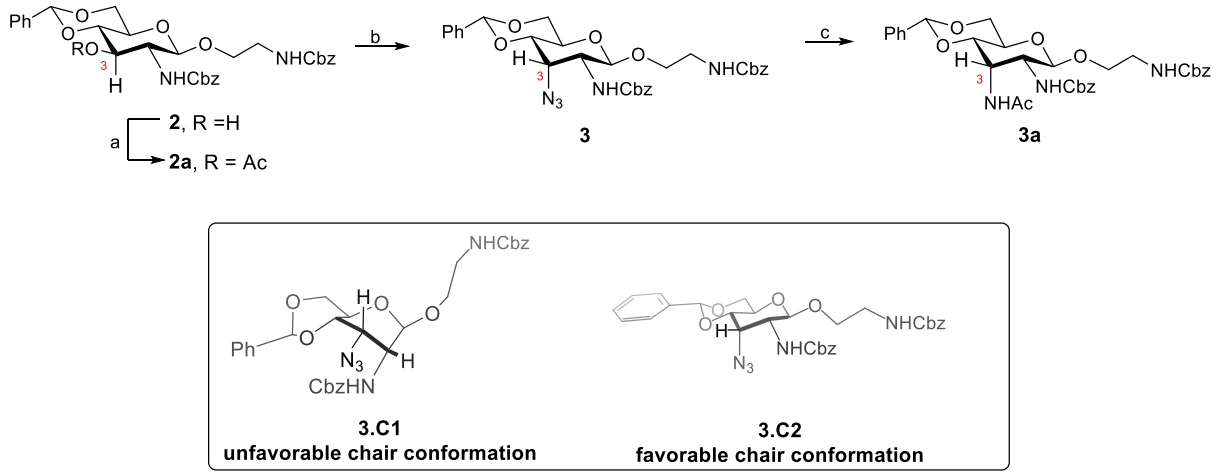

[a]Reagents and conditions: (a) Ac_2O, DMAP, TEA, CH_2Cl_2; 26%; (b) DPPA, DIAD, Ph_3P, TEA, THF; 79%; and (c) (i) Me_3P, 0.1 N NaOH, THF and (ii) Ac_2O, DMAP, TEA, CH_2Cl_2, 76% (2 steps).

Scheme 2. Synthesis of DAP TLR4 Agonists 8a−c[a]

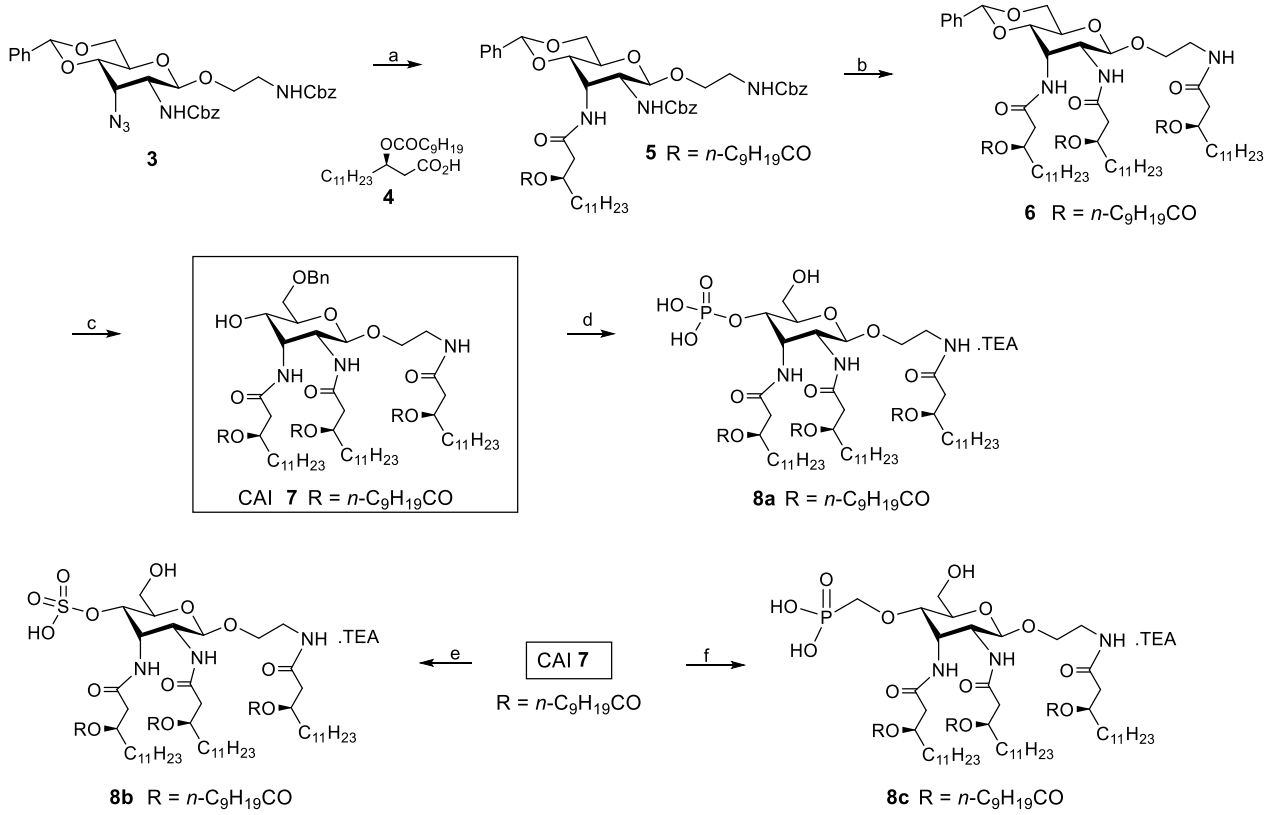

[a]Reagents and conditions: (a) (i) Me_3P, 0.1 N NaOH, THF, and (ii) EDC.MeI, **4**, CH_2Cl_2; 76% (2 steps); (b) (i) Pd/C, pyr, H_2(g), THF:MeOH (4:1) and (ii) EDC.MeI, **4**, CH_2Cl_2; 66% (2 steps); (c) TFA, $NaCNBH_3$, CH_2Cl_2; 93%; (d) (i) $(BnO)_2PNi\text{-}Pr_2$, DCI, CH_2Cl_2 then H_2O_2, (ii) Pd/C, H_2(g), THF, and (iii) TEA; 62% (3 steps); (e) (i) SO_3.TEA, DMF, (ii) $Pd(OH)_2$/C, H_2(g), THF:MeOH (4:1), and (iii) TEA, 55% (3 steps); and (f) (i) $TfOCH_2PO(OBn)_2$, LiHMDS, THF, (ii) Pd/C, H_2(g), THF, and (iii) TEA, 27% (3 steps).

following intranasal administration and mediate protection against a lethal influenza challenge in a dose-dependent manner.

RESULTS AND DISCUSSION

Chemistry. Ester hydrolysis has been a major issue in the synthesis of TLR4 agonists, leading to lower yields, difficult preparations, in-process impurities, and reduced stability/shelf life as seen with synthetic TLR4 agonist AGPs **1a−c**; especially the hydrolysis of the 3-*O* secondary ester (data not shown), which is likely facilitated by its proximity to the phosphate on the C-4 position. On the other hand, the amide moiety is a common functional group present in many biologically active molecules, including peptides and proteins and clinically approved, synthetic, experimental, and naturally derived drug molecules.

https://doi.org/10.1021/acs.jmedchem.3c00724
J. Med. Chem. 2023, 66, 13900−13917

Scheme 3. Synthesis of DAPs 17a−c[a]

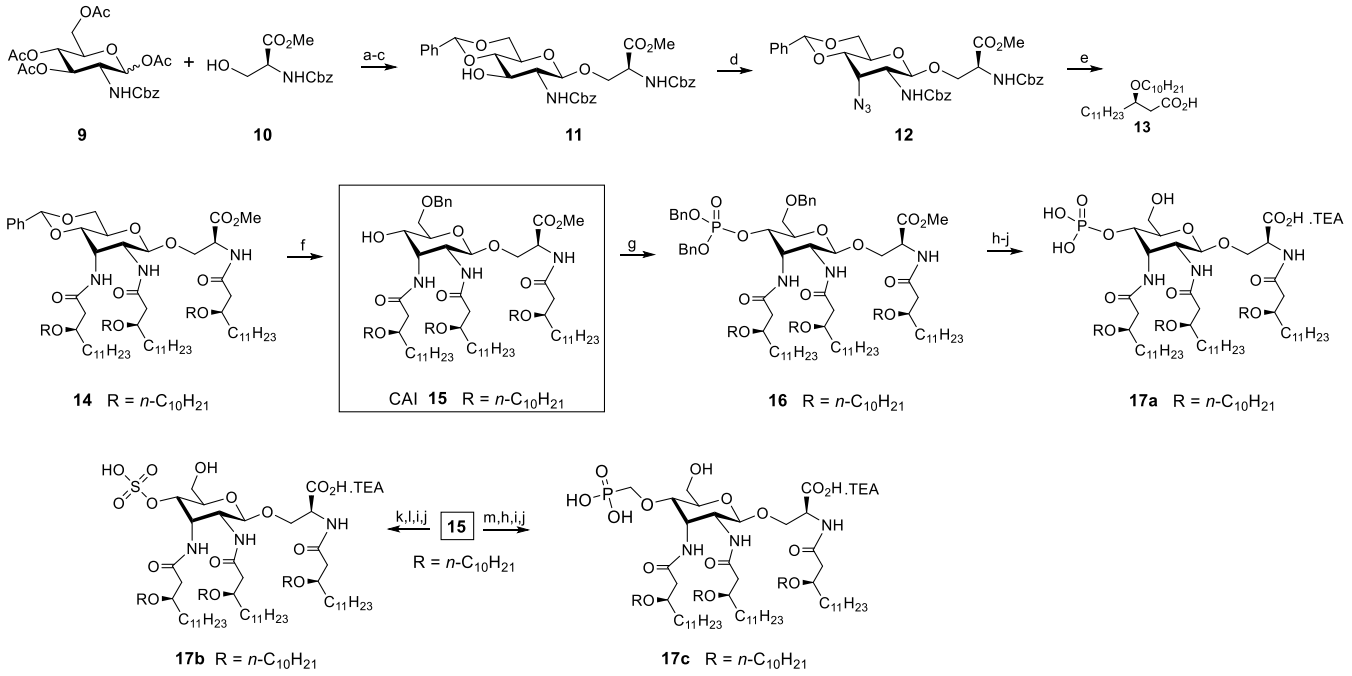

[a]Reagents and conditions: (a) $BF_3{\cdot}Et_2O$, CH_2Cl_2, quantitative; (b) $Mg(OCH_3)_2$, CH_3OH, 44%; (c) $PhCHOMe_2$, CSA, CH_3CN, 75%; (d) DPPA, DIAD, PPh_3, TEA, THF, 78%; (e) (i) Pd/C, H_2(g), THF and (ii) **13**, EDC.MeI, CH_2Cl_2, 63% (2 steps); (f) TFA, $NaCNBH_3$, CH_2Cl_2, 84%; (g) $(BnO)_2PNiPr_2$, DCI, CH_2Cl_2 then H_2O_2, 93%; (h) Pd/C, H_2(g), THF; (i) LiOH, THF-H_2O, 41% (**17a**), 63% (**17b**), 11% (**17c**); (j) TEA salting; (k) SO_3.TEA, DMF, 98%; (l) $Pd(OH)_2$/C, TEA, H_2(g), THF-CH_3OH (4:1), 60%; and (m) $(BnO)_2POCH_2OTf$, LHMDS, THF, 36%.

Correspondingly, the amide bond has a prominent role in drug design and development to allow an increase in potency, enhanced selectivity, improvements of pharmacokinetic properties, and the acquisition of novel chemical space to secure intellectual property. In this respect, an equatorial amide bond on the 3-position of the aforementioned TLR4 agonists is a rational modification to the labile equatorial 3-ester, ergo more resistant to hydrolytic cleavage. However, such a carbohydrate entity with a 3-equatorial amide is already present in nature, as exemplified in *Leptospira interrogans* lipid A.[46] Additionally, converting the 3-equatorial hydroxyl group to the corresponding 3-equatorial amino group would require 4 sequential functional transformations, which is not necessarily efficient.[47−49] The natural availability of LPS disaccharides containing 3-equatorial amide groups and the synthetic complexity of incorporating either a 3-equatorial amide or a hydrolytically susceptible 3-axial ester[50] led us to explore the incorporation of the more stable and synthetically more accessible 3-axial amide.

The synthesis of compounds **8a−c** and **17a−c** bearing the nonhydrolyzable 3-amide bond is outlined in Schemes 2 and 3. Our synthetic strategy exploited an orthogonally protected glucosamine by blocking the 4- and 6-positions as a 4,6-di-*O*-benzylidene group (**2** and **11**, Schemes 2 and 3, respectively), a well-established strategy in the synthesis of lipid A mimetics.[51,52] The orthogonal protected glucosamine created a structural motif amenable to further modifications, specifically the incorporation of the 3-axial azido group early on and late-stage derivatization at the fourth position. Prior to inverting the chiral center at the C-3 position, we determined the chemical shift of H-3 glucosamine for both **2** and its corresponding acetylated **2a** compound (Scheme 1) through a series of ^1H and $^1H-^1H$ COSY NMR experiments. The signal corresponding to H-3 in **2** appeared as a broad singlet at 3.68 ppm (Figures S1 and S2). The chemical shift of the H-3 signal in **2** was further supported by the strong down-shield shift of this signal in **2a** appearing as a triplet ($J_{2,3} \cong J_{3,4}$ = 10 Hz) at 5.21 ppm, as well as the clear correlation of H-3 with H-2 and H-4 in the $^1H-^1H$ COSY spectrum (Figures S4 and S5). The signal and chemical shift of glucosamine H-3 in **2** are comparable with those reported by Emmadi and Kulkarni for their 4,6-*O*-benzylidene-2-deoxy-2-(2,2,2-trichloroethoxycarbonylamino)-1-thio-β-D-glucosamine.[47] Once the H-3 signal in **2** was determined, we proceeded with the chiral center inversion.

In contrast to double inversion, e.g., the Lattrell-Dax approach (four synthetic steps),[53] we exploited the Mitsunobu reaction, a well-known single-step approach that proceeds under mild and neutral conditions compatible with a wide range of functional groups to convert the 3-hydroxyl group to 3-azide with inversion of configuration.[54,55]

We first synthesized compound **8a**, starting from the orthogonally protected advanced intermediate **2**[54] (prepared in 7 steps and 28% overall yield), as shown in Scheme 2. A first attempt to convert the equatorial 3-hydroxyl in **3** to a mesylate before performing a SN2 displacement of the resulting mesylate with sodium azide NaN_3[49] failed to provide the desired mesylate. Hence, we opted for the single-step approach using the Mitsunobu reaction.

The Mitsunobu reaction on **2** was carried out with diphenyl phosphoryl azide (DPPA), diisopropyl azodicarboxylate (DIAD), and triphenylphosphine delivering the inverted axial 3-azido intermediate **3**. The inclusion of the azide provided the protected 2,3-deoxy-3-azido-2-amino allose scaffold set to incorporate the acyl chains.

In an effort to determine the configuration of C-3 following the Mitsunobu reaction, we attempted to produce compound **3** as a crystalline solid; however, these attempts only resulted in

https://doi.org/10.1021/acs.jmedchem.3c00724
J. Med. Chem. 2023, 66, 13900−13917

producing powder not amenable to X-crystallography. We then reverted to a combination of NMR experiments and molecular modeling. The ^{1}H NMR spectrum of **3** revealed the H-3 signal strongly deshielded at 4.31 ppm, overlapping with H-6a (Figure S6). This signal is characteristic of the *allo* configuration, again similar to what Kulkarni reported with 4,6-*O*-benzylidene-2-deoxy-2-(2,2,2-trichloroethoxycarbonylamino)-1-thio-β-D-allosamine.[47] To better determine the *J* coupling value of the inverted C-3, Staudinger reduction of azide **3** to 3-amine and acetylation (Scheme 1) effectively shifted the H-3 signal in **3a** to 4.71 ppm as a narrow singlet, indicating a very small $J_{2,3} \cong J_{3,4}$ coupling corresponding to an equatorial H-3, thus confirming the *allo* configuration (Figures S8 and S9). These characteristics are in line with reported chemical shifts for allosamine derivatives.[47,50,56]

While we established the *allo* configuration of **3**, the SN2 displacement of equatorial 3-OH to its axial 3-N_3 can potentially result in two chair confirmations **3C.1** or **3C.2**, as shown in Scheme 1. The alternate conformation **3C.1**, in which the C-3 azide is in pseudoequatorial orientation and both C-2 NHCbz and C-4 O−CH of benzylidene are in pseudoaxial orientation, would be unfavorable as 1,3-diaxial repulsion (dipole−dipole repulsion) between C-2 and C-4 could occur. This was further supported by energy minimization calculation performed on both **3C.1** and **3C.2** using Chem3D modeling with **3C.2** having the lowest energy value (Table S1 and Figure S49).

Having confirmed the chirality of C-3 following the Mitsunobu reaction, we then proceeded with the synthesis by initially performing a one-pot selective azido reduction and Cbz group deprotection in the presence of the benzylidene acetal via hydrogenation with Pd/C and a trace of pyridine, followed by carbodiimide-mediated acylation with (*R*)-decanoyloxytetradecanoic acid **4**,[24] to obtain the triacyl intermediate **6**. The addition of a trace amount of pyridine poisoned the Pd catalyst, preventing the reductive cleavage of the benzylidene ring. Because of inconsistent yields, we then investigated a two-step transformation involving a Staudinger reaction[57,58] on **3**, followed by a carbodiimide-mediated monoacylation using 1-(3-(dimethylamino)propyl)-3-ethylcarbodiimide methiodide (EDC.MeI) with acid **4** to afford the monoacyl intermediate **5**. The Cbz groups were then selectively removed in the presence of the benzylidene acetal using catalytic hydrogenolysis with Pd/C and trace amounts of pyridine. Subsequent *N*,*N*-diacylation with **4** furnished the desired triacyl intermediate **6**. Regioselective reductive ring opening of the benzylidene group in **6** led to the common advanced intermediate (CAI) 6-*O*-benzyl **7**. Subsequent phosphorylation/oxidation at the 4-positon, followed by benzyl deprotection and triethylamine (TEA) salting afforded the first desired DAP compound **8a**.

To date, many naturally occurring lipid A cores, detoxified (e.g., MPLA) and synthetic lipid A mimetics (e.g., GLA and AGPs), encompass the 2-amino-2-deoxy-glucose (glucosamine) scaffold in the carbohydrate backbone and contain the classical and yet labile ester bond at the 3-position. Replacing the ester with an amide in compound **8a** represents a unique, first-in-class synthetic lipid A mimetic with a diamino allose core making way for the development of a novel series of TLR4 ligands and expanding the landscape for existing synthetic TLR4 agonists.

In addition to the labile 3-ester group, classical lipid A-based natural and synthetic TLR4 agonists possess a labile phosphate group at the 4-position. The 4-phosphate group is essential for TLR4 activity because of its interaction with positively charged residues in TLR4 and MD2 in the TLR4−MD2 complex.[59] Phosphate esters are chemically stable in aqueous solutions at physiological pH but are easily hydrolyzed by phosphatases in vivo.[60] They can also undergo cleavage and/or migration to the 6-position during synthesis, leading to less active compounds (unpublished results). In an effort to further improve the stability of these synthetic TLR4 ligands, we investigated the effect of more stable phosphate bioisosteres on TLR4 activity by synthesizing compounds **8b** and **8c** bearing sulfate or methylphosphonate groups at the 4-position, respectively. Sulfate groups are approximately tetrahedral, hence similar in shape to phosphate groups, highly acidic,[61] and fully ionized at physiological pH. Methylphosphonates are also geometrically and electronically similar to phosphates.[62] Both of these functional modifications onto sugars have been reported: sulfation is commonly involved as a post-glycosylation modification of carbohydrates or glycans,[63] and methylphosphonates have been incorporated in oligonucleotides, metabolically stable analogues of conventional DNA.[64] However, the inclusion of a methylphosphonate on the C-4 position of lipid A mimetics has not been reported. Accordingly, the two phosphate bioisosteres were introduced at the 4-position of CAI **7**; compound **8b** was obtained in three steps by sulfation,[65] subsequent benzyl deprotection, and TEA salting, and compound **8c** was prepared by alkylation with (bis(benzyloxy)-phosphoryl)methyl trifluoromethanesulfonate,[66] followed by benzyl deprotection and TEA salting.

To further extend the potency range of our DAPs family, we next sought to introduce the 3-amide bond to the synthetic TLR4 agonist **1c** containing a carboxyl group (bioisosteric with the 1-phosphate moiety of lipid A).[23,26] We previously reported that replacing the secondary acyl chain **1b** with a secondary alkyl chain **1c** does not affect TLR4 potency.[25] The synthesis of **17a** was accomplished by stereoselective β-glycosylation of the glycosyl donor **9** and *N*-Cbz L-serine methyl **10** using the directing *N*-2-benzylformate (Cbz) group, followed by a series of standard protecting group manipulations to produce intermediate **11** (Scheme 3).

Treatment of **11** with the aforementioned Mitsunobu conditions incorporated the inverted azido group on the 3-position in **12**. Although the L-seryl aglycon added complexity to the ^{1}H NMR spectra, the signal corresponding to H-3 in **11** at 3.75 ppm (partially obscured by the CH_3 ester protons) was deshielded to 4.33 ppm in **12** overlapping with the H-6a signal, again characteristic to the *allo* configuration (Figures S22 and S24). Initial attempts to convert the azide to the amine using the Staudinger reaction failed. Alternatively, catalytic hydrogenolysis of **12** followed by EDC-mediated *N*,*N*,*N*-triacylation with the requisite (*R*)-3-decyloxytetradecanoic acid **13**[24] afforded the triacyl intermediate **14** with no loss of the benzylidene acetal group. Regioselective opening of the benzylidene acetal and subsequent phosphorylation produced compound **16**. The remaining transformations included sequential hydrogenolysis, hydrolysis with LiOH, and TEA salting to obtain the desired DAP monosaccharide **17a**.

The 6-benzyl intermediate **15** served as a common advanced intermediate to replace the labile phosphate group with the more stable sulfate and methylphosphonate bioisosteres. The sulfate bioisostere **17b** was obtained from **15** via a four-step sequence involving sulfation, hydrogenolysis, hydrolysis, and TEA salting. Removal of the benzyl group from the 6-position by hydrogenolysis required more basic conditions, e.g., $Pd(OH)_2$/C and TEA.

https://doi.org/10.1021/acs.jmedchem.3c00724
J. Med. Chem. 2023, 66, 13900−13917

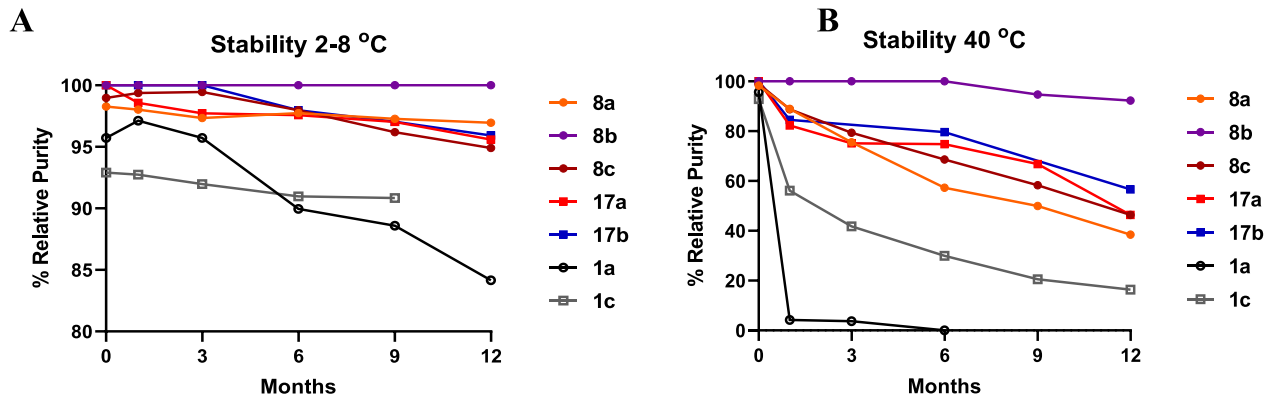

Figure 2. Stability of aqueous formulations of aminoethyl glycosides **8a−c** and seryl glycosides **17a−b** against corresponding benchmarks **1a** and **1c** at (A) 2−8 °C and (B) 40 °C.

We followed a similar synthetic sequence to incorporate the methylphosphonate to prepare **17c**; however, the yields and purification in each step (alkylation of **15** with (bis(benzyloxy)-phosphoryl)methyl trifluoromethanesulfonate, followed by hydrogenolysis and hydrolysis) were low and challenging, resulting in limited production of **17c**. Consequently, the stability of **17c** was not investigated. In addition, the limited amount of **17c** prevented the acquisition of highly resolved ^{1}H and ^{13}C NMR spectra (Figures S36 and S37).

All new compounds in the DAP series were converted to the TEA salt and were isolated in >95% purity (determined by RP-HPLC, Figures S38−S43).

Stability. Since our primary objective was to improve the thermostability of AGPs, we evaluated compounds **8a−c** and **17a−b** against known benchmarks **1a−c** for stability when formulated in isotonic nonbuffered 2% glycerol-based formulations stored at 2−8 and 40 °C for 12 months. Because of limited availability, the stability study on **17c** was not conducted.

To evaluate the stability of the new compounds, the percent relative purity in the formulations at different time points was determined by RP-HPLC and the main degradants identified by LCMS. In general, compounds **8a−c** and **17a−b** were found to maintain high purity (>95%) at 2−8 °C relative to the corresponding benchmarks **1a** and **1c** over 12 months, demonstrating the introduction of the axial 3-amide on the 3-position improved stability (Figure 2A). At 40 °C, all compounds tested showed different rates of degradation; however, series **8** and **17** had the lowest rate of degradation relative to their benchmarks; in particular, the sulfate analogue **8b** underwent less than 10% degradation after 1 year at 40 °C. Not surprisingly, the loss of the 3-acyl was detected in **1a** and **1c** as early as 3 months and 1 month at 2−8 and 40 °C, respectively, as revealed by LCMS analysis (data not shown). While no loss of the 3-acyl was noted in **8a−c** and **17a−c**, LCMS analysis indicated loss of the divalent phosphate group on the 4-position in **8a** and partial hydrolysis among the secondary acyl chains in **8a** and **8c**. Interestingly, the introduction of the monovalent sulfate group altered the physicochemical properties of **8b**; neither hydrolysis of the sulfate group nor the secondary acyl chains were observed at 2−8 °C, and only partial (8%) hydrolysis of the secondary acyl chains was observed at 40 °C after 12 months. Similarly, the sulfate analogue **17b** was more stable than the corresponding phosphate analogue **17a**. The major degradant in **17a−b** resulted from the cleavage of the glycosidic bond detected in the accelerated studies (data not shown).

Biological Activity. Because of the reported species-specific recognition of some lipid A analogues,[67] the six new compounds were evaluated for murine (m) and human (h) TLR4 activity and relative potency in cell lines and primary human cells, and compared to the known TLR4 agonist benchmarks MPLA, GLA, **1a**, and **1c** (Table 1 and Figure S44).[34,42,68,69] Human and murine TLR4 potency and specificity were first evaluated using HEK293 cells stably transfected with either hTLR4 or mTLR4 and the NF-kB SEAP (secreted embryonic alkaline phosphatase) reporter from InvivoGen (San Diego, CA). These assays measure NF-kB-mediated SEAP production following TLR4-specific activation. Human embryonic kidney (HEK) null cells (HEK cells containing the NF-kB reporter without the TLR4 receptor) were used as negative controls to confirm the receptor specificity of the compounds. The species specificity and relative

Table 1. NF-κB Response of HEK293-mTLR4 and hTLR4 Cells and MIP-1β Induction from RAW264.7 and MM6 Cells Stimulated for 24 h with Compounds 8a−c and 17a−c and Corresponding Benchmarks MPLA, GLA, 1a, and 1c[a]

	HEK293 cells		RAW cells	MM6 cells
compounds	mTLR4 EC_{50}, nM (95% CI)	hTLR4 EC_{50}, nM (95% CI)	MIP-1β EC_{50}, nM (95% CI)	MIP-1β EC_{50}, nM (95% CI)
MPLA	6.54 (4.30−10.03)	246.0 (146.1−553.6)	3.73 (2.86−5.0)	6.37 (na)
GLA	1.4 (0.92−2.15)	6.23 (5.61−6.94)	0.49 (0.35−0.67)	0.99 (0.51−2.12)
1a	0.43 (0.25−0.75)	172.7 (139.8−217.0)	0.48 (0.35−0.64)	6.75 (4.03−12.06)
1c	0.005 (0.002−0.02)	0.93 (0.68−1.26)	0.015 (0.010−0.023)	0.06 (0.02−0.14)
8a	0.37 (0.25−0.53)	91.9 (75.7−111.5)	0.26 (na−0.38)	1.65 (0.71−3.92)
8b	2.64 (0.82−7.6)	449.0 (378.8−541.0)	0.31 (0.24−0.40)	39.5 (24.01−71.59)
8c	0.50 (0.30−0.82)	68.2 (55.2−84.6)	0.09 (0.07−0.12)	1.49 (1.12−1.99)
17a	0.15 (0.03−0.59)	7.86 (5.46−11.04)	0.02 (0.01−0.06)	0.38 (0.25−0.56)
17b	0.68 (0.25−1.59)	26.3 (16.7−40.5)	0.04 (0.03−0.05)	0.65 (0.45−0.94)
17c	0.19 (0.06−0.51)	7.71 (5.19−11.33)	0.03 (0.02−0.05)	0.26 (0.19−0.34)

[a]EC50 and 95% CI values were calculated by analyzing data using nonlinear regression (curve fit) and fitting data to a four-parameter (variable response), agonist concentration−response model in Prism.

https://doi.org/10.1021/acs.jmedchem.3c00724
J. Med. Chem. 2023, 66, 13900−13917

potency of the compounds were also assessed through cytokine induction (MIP-1β) in murine RAW264.7 and human monocytic Mono-Mac-6 (MM6) cell lines (Figure S45). To further explore the potential of these compounds for human use, freshly isolated PBMCs were used to confirm the activity in primary cells and assess the cytokine induction (MIP-1β, TNFα, IL-1β, and RANTES) of targeted compounds **8a−c** and **17a−c** and benchmarks (Table 2 and Figure S46). Compounds **1a−c** and **17a−c** and benchmarks were formulated at 2 mg/mL in 2% aqueous glycerol, as previously described.[27]

Table 2. MIP-1β, IL-1 β, TNFα, and RANTES Induction in PBMC Stimulated for 20 h with 8a−c and 17a−c and Benchmarks[a]

	PBMC EC_{50} (nM)			
compounds	MIP-1β	TNFα	IL-1β	RANTES
MPLA	23.68	199.62	42.41	31.49
GLA	0.76	10.41	2.11	1.92
1a	1.94	53.75	2.62	1.26
1c	0.010	0.26	0.028	0.014
8a	1.61	28.00	8.77	3.68
8b	2.87	116.27	20.36	7.01
8c	1.23	34.58	2.69	1.78
17a	0.13	2.60	0.28	0.14
17b	0.24	6.88	0.97	0.46
17c	0.11	1.33	0.20	0.13

[a]EC50 values are calculated by analyzing data into nonlinear regression (curve fit) and fitting data to a four-parameter (variable response), agonist concentration−response model in Prism, one representation of three independent donors. Error bars included in Figure S46.

Compounds **8a−c** were initially evaluated against the benchmarks MPLA, GLA, **1a**, and **1c** for human and murine TLR4 specificity, relative potency, and cytokine induction (Table 1) to investigate the effects of converting the 3-equatorial ester to the 3-axial amide and replacing the phosphate on the 4-position with bioisosteres. Compounds **8a−c** retained TLR4 activity in both human and murine HEK293 reporter assays, with improved potency relative to MPLA (2.7 to 3.6 and 2.7 to 15-fold in the human and murine systems, respectively) and comparable potency to **1a** (Table 1 and Figure S44). Upon closer examination, the monovalent sulfated compound **8b** exhibited lower relative potency in the HEK293 reporter assay than the two divalent phosphate-containing compounds **8a** and **8c** (Table 1). The crystal structure of LPS in the TLR4-MD2 complex shows the 1- and 4- phosphate groups of LPS interact with a cluster of positively charged residues in the complex.[59] Hence, it is possible that the loss of a valence charge in **8b** on the 4-position contributes to a slightly weaker ionic/hydrogen bond interaction with the lysine or seryl residues in the TLR4/MD-2 complex.

Analogues **17a−c** also demonstrated potent TLR4 agonist activity with equivalent or improved activity in comparison to MPLA or GLA but were less active than the corresponding AGP **1c** (Table 1 and Figure S44). Similar to previously reported in the AGP series of synthetic TLR4 ligands,[23,26] **17a−c** with L-seryl aglycon were more potent than their ethylamine counterparts **8a−c**. None of the compounds elicited signaling via NF-kB when tested in the HEK null cell line, further confirming their TLR4 specificity (data not shown).

The new compounds were also evaluated for cytokine induction in both murine RAW264.7 and human monocytic MM6 cell lines. The new compounds showed similar trends to what was observed in the HEK293 reporter assay. The incorporation of the 3-axial amide in the aminoethyl glycosides **8a−c** and the seryl glycosides **17a−c** and substitution of the phosphate with the sulfate and methylphosphonate groups in **8b−c** and **17b−c**, respectively, did not reduce TLR4 activity in these cell lines (Table 1 and Figure S45). Series **8a−c** and **17a−c** exhibited increased potency relative to MPLA and were equivalent to GLA. In contrast to what was observed in the HEK reporter assays, the sulfate group in **8b** and **17b** did not exhibit reduced TLR4 potency in RAW264.7 and MM6 cell lines but rather were found to be equivalent to **8a−c** and **17a−c** (Table 1 and Figure S45).

To further explore the potential of these compounds for human use and the effect of the structural changes on biological activity, cytokine induction from freshly isolated PBMC was assessed with compounds **8a−c** and **17a−c** and compared with the benchmark TLR4 ligands MPLA, GLA, **1a**, and **1c** (Table 2 and Figure S46). Each of the new TLR4 ligands induced cytokines (MIP-1β, IL-1β, TNFα, and RANTES) with equivalent or increased potency in relation to MPLA and GLA. As expected, the seryl series was more potent than the ethylamine **8a−c** series. The monovalent sulfate group in **8b** and **17b** had minimal impact on potency in relation to **8a−c** and **17a−c**, respectively. Compound **17a** was about 10-fold less potent than **1c** in inducing MIP-1β, IL-1β, TNFα, and RANTES in PBMCs, most likely a result of the conversion of the equatorial ester to the axial amide. These trends were shared among the three donors tested, although donor-to-donor differences in terms of peak level and minimum effective concentration were observed. Table 2 is representative data from one out of three independent donors (Figure S46). PrestoBlue assays were performed to assess cytotoxicity in PBMCs. Both representative DAP compound **17a** and known synthetic TLR 4 agonist **1b** did not affect cell viability even at higher concentrations (up to 10 μg/mL) (Figure S47).

In summary, the in vitro results indicated that (i) replacing the labile 3-ester group with a stable 3-amide group, (ii) switching the configuration at the 3-position from an equatorial substituent to an axial substituent, and (iii) replacing the 4-phosphate with bioisosteres did not negatively impact TLR4 activity or cytokine induction while having a profound positive impact on compound thermostability.

Due to their ability to stimulate innate immunity and enhance downstream adaptive immune responses, TLR4 agonists have emerged as an attractive target for the development of vaccine adjuvants. A number of studies have described the ability of TLR4 agonists to mediate distinct responses in mouse and human cells and to support the differentiation of T helper Th1 or Th2 immune responses.[70,71] Unlike alum, which tends to generate Th2 responses, TLR4 agonists including MPLA and AGPs facilitate Th1 polarization, characterized by a qualitative shift in the immune response, significantly boosting IgG2a antibody titers when coadministered with a vaccine antigen(s).[29,72]

In this respect, our novel series of TLR4 agonists were evaluated for their ability to enhance humoral immunity to a monovalent detergent-split influenza vaccine following intramuscular vaccination in mice. Compounds **8b** and **17a−c** were compared to the TLR4 agonist **1c** in a murine model of influenza vaccination. BALB/c mice (10 mice/group, 7−9 weeks old)

https://doi.org/10.1021/acs.jmedchem.3c00724
J. Med. Chem. 2023, 66, 13900−13917

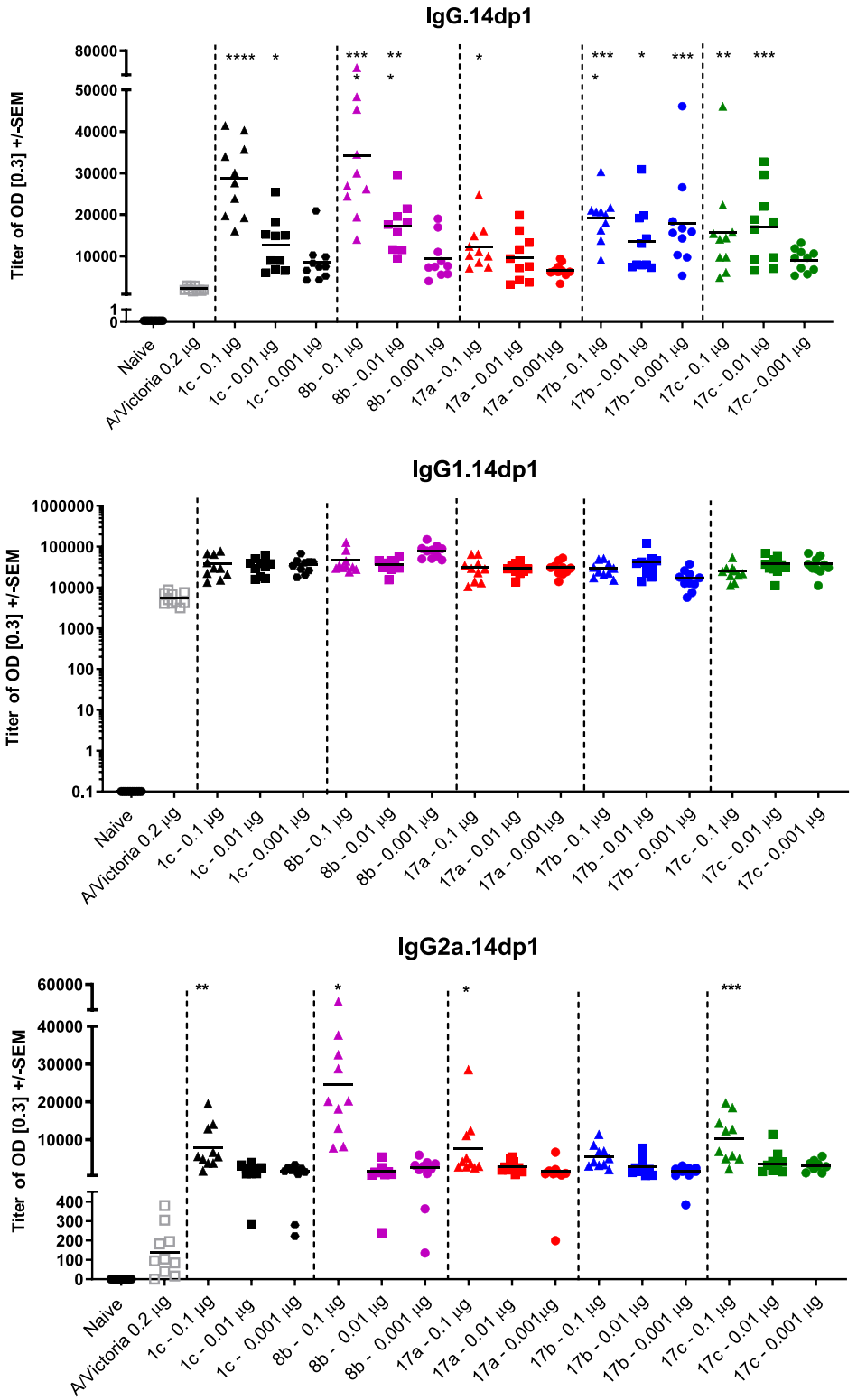

Figure 3. A/Victoria antigen-specific IgG, IgG1, and IgG2a antibodies induced 14 days post-primary vaccination. Statistical significance determined by a one-way ANOVA (GraphPad Prism 7): asterisk indicates significance compared to the A/Vic alone group (gray "□") where *$p \leq 0.05$, **$p \leq 0.01$, ***$p \leq 0.001$, ****$p \leq 0.0001$.

were vaccinated twice intramuscularly on days 0 and 14 with 0.3 μg HA equivalent monovalent detergent-split A/Victoria/210/2009 (H3N2) and 0.001, 0.01, or 0.1 μg of each TLR4 agonist. Serum was harvested on days 14 [14 days post-primary vaccination (14dp)] and 28 [14 days post booster (14dp2)], (Figure S48), for assessment of influenza-specific humoral immunity. Influenza-specific serum IgG and IgG1 antibody titers were significantly ($P < 0.05$) increased by **8b** and **17a−c** in a dose-dependent manner 14 days post-primary vaccination and were similar to **1c**, compounds **8b**, **17a**, and **17c** significantly increased IgG2a titers in a dose-dependent manner 14 days post-primary vaccination (Figure 3). Following the booster

https://doi.org/10.1021/acs.jmedchem.3c00724
J. Med. Chem. 2023, 66, 13900−13917

vaccination (14 days postsecondary vaccination), all adjuvanted groups exhibited increased average IgG, IgG1, and IgG2a titers compared to the nonadjuvanted A/Vic control (14dp2; Figure S48). This study confirms that the structurally unique series **8a−c** and **17a−c** function as adjuvants and enhance humoral immunity to a coadministered antigen. Additionally, no signs of overt toxicity or local reactogenicity were noted at any point during the study. These data provide strong evidence that the DAP TLR4 agonists are safe and effective vaccine adjuvants.

Previously, we (and others) reported that synthetic TLR4 ligands function as both vaccine adjuvants and stand-alone immunomodulators capable of inducing a window of nonspecific resistance against subsequent influenza virus infection.[29,31,34,35] Above, we demonstrated the ability of the novel TLR4 agonists **8b** and **17a−c** to act as adjuvants when coadministered with an antigen. We also evaluated the induction of innate immunity (cytokines) by these compounds in vitro. Next, we explored the ability of the DAP TLR4 agonists to induce nonspecific resistance (innate immune-mediated clearance) to infectious challenges, thereby acting as stand-alone prophylactic immunotherapeutics. Mice (8 mice/group) were treated intranasally with the indicated dose of **17a** or **1c** and then challenged 48 h later with a 1LD50 dose of mouse-adapted A/Hong Kong/1/68 (H3N2; A/HK/68), as previously described.[35] As expected, most of the naive (vehicle-treated) mice succumbed to the 1LD50 influenza virus challenge with 80% mortality by day 10 following the challenge (Figure 4).

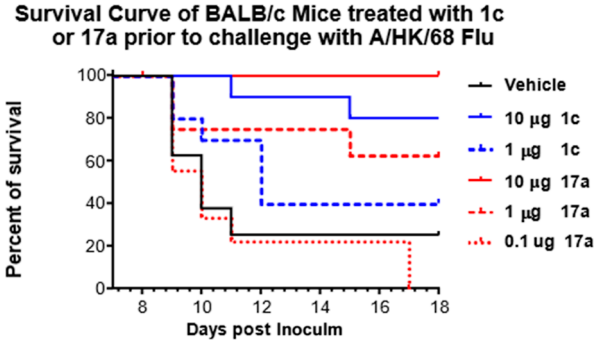

Figure 4. Survival curve of Balb/c mice (8 mice/group) received an indicated dose of **1c** and **17a** in 2% glycerol in water by intranasal administration 2 days prior to influenza challenge (1LD50, A/HK/68). Survival was recorded for 18 days post-viral challenge following IACUC-approved humane euthanasia end points.

Notably, **17a** provided protection in a dose-dependent manner, with 100% and 60% survival at the 10 and 1 μg doses, respectively, while **1c** afforded 80 and 40% survival at the same doses (Figure 4). No toxicity was observed upon administration of **17a** or **1c**. These preliminary data demonstrate that the new DAP TLR4 agonist **17a** can induce nonspecific resistance and confer protection against the influenza virus. This influenza model also highlights the capacity of the DAP TLR4 agonists for stimulating early innate immune responses limiting the initial spread of a respiratory infection.

As observed from the immunological profile of **17a**, the change in the stereochemistry at the C-3 position appears to cause some reduction in potency in the HEK, RAW, MM6, and PBMC in vitro systems when compared to the benchmark TLR4 agonist **1c**. However, **17a** has a notably improved activity as compared to **1c** in the influenza challenge study. We sought to perform molecular docking on the DAP series and representative benchmark **1c** to shed light on the activity.

Molecular Docking Analysis. In the present work, we have replaced the classical equatorial 3-ester group with a more stable 3-amide group in axial orientation, resulting in a novel series of TLR4 agonists known as DAPs. To better understand the effect of the difference in axial/equatorial conformation, we used Chem3D to perform a preliminary computational analysis of the representative compound **17a** and its equatorial version (**17aEQ**), in which the amide functionality is in an equatorial orientation. Energy minimization of **17a** and **17aEQ** revealed both monosaccharides are in a chair conformation (Figure S50); however, the energy values slightly vary between the two conformations culminating in the total energy of **17aEQ** (87.0923 kcal/mol) to be slightly less than **17a** (90.1260 kcal/mol) (Table S2).

Previously, we demonstrated that the C2 symmetry of AGPs, synthetic TLR 4 agonists, allowed them to possibly enter the MD-2 pocket in a LPS-like (agonist) or in an Eritoran-like (antagonist, 180° rotation) orientation modulating the immune response.[28] Given the pseudo-C2 symmetry of the DAP series, it is likely that the DAP ligands could be inserted into the pseudosymmetry of MD2 in both orientations as well.

To rationalize the experimental results observed with our new TLR4 agonists and to gain an understanding of their binding modes, molecular docking of compounds **8a−c** and **17a−c** was performed using the AutoDock Vina[73,74] algorithm utilizing the AMDock GUI.[75] The molecules were docked in the pseudosymmetrical huTLR4-MD-2 complex (PDB: 3FXI) using ligand protonation at 7.4 pH from low energy conformations calculated using the steepest descent method with AMBER/GAFF force

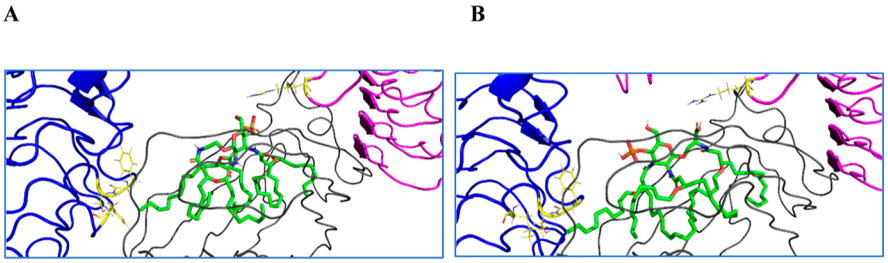

Figure 5. Predicted favorable binding modes of **8b** (A) in Eritoran-like and **17a** (B) in LPS-like orientations and interacting at the dimerization interface with TLR4* ectodomain and its TLR4-MD-2 complex, i.e., TLR4-MD2-TLR4* (PDB: 3FXI). TLR4* ectodomain, MD-2, and TLR4 are shown in blue, gray, and purple, respectively. The DAP molecule bound to the hydrophobic cavity of MD-2 is shown as a ball and stick with C, N, O, P, and S atoms shown as cyan, blue, red, purple, and yellow, respectively, and side chains of certain amino acid residues participating in interactions (<4 Å) between TLR4*, MD-2, TLR4, and DAP, are shown in yellow.

https://doi.org/10.1021/acs.jmedchem.3c00724
J. Med. Chem. 2023, 66, 13900−13917

fields. PyMOL 2.5.2 was used to visualize docked molecules, as illustrated in Figure 5, and to measure ligand−protein interaction distances.

The docking calculations show that all 6 DAP ligands are theoretically able to interact within the hydrophobic pocket of MD-2 as well as with various charged residues on either the TLR4/TLR4* ectodomain. Further, relevant poses of all 6 DAP ligands exhibit binding affinities within the binding complex (PDB:3FXI) ranging from −7.0 to −7.6 kcal/mol. The possibility of a DAP inserted into the MD-2 pocket in either orientation is further supported by molecular modeling studies, as represented in Figure 5. Interestingly, the most favorable docked poses of **8b** and **8c** in the MD-2 pocket reflect an Eritoran-like orientation, with the 4-sulfate of **8b** and 4-methylphosphonate of **8c** engaging in ionic interactions (≤4 Å) with R264 in TLR4 (Figures 5 and S51). In contrast, docking modeling of **17a−c** inserted into the MD-2 pocket in a LPS-like orientation reveals the carboxyl moiety of the L-seryl aglycon interacting primarily with R264 of TLR4 and the C4-anionic moiety (phosphate, sulfate, and methylphosphonate) interacting possibly through H-bonding with E439* on the TLR4* ectodomain. Compound **8a** is also docked into the MD-2 pocket in a LPS-like orientation, but its C-4 phosphate appears to be exposed to the solvent at the interface of the TLR4* ectodomain. Regardless of orientation in the MD-2 pocket, the terminus lipid chain of the secondary acyl at the 3-position on the sugar or the aglycon is oriented at the interface of the TLR4* ectodomain and is sufficiently proximal to form hydrophobic interactions with residues, namely, F440*, L444*, and F463* (Figures 5 and S51).

Using the same parameters, we also docked the benchmark synthetic TLR4 agonist **1c** in the pseudosymmetrical huTLR4-MD-2 complex (PDB: 3FXI) (Figure S52), revealing a preferential binding mode of the Eritoran-like orientation in contrast to its 3-axial amide analogue **17a**. The binding of **1c** in the huTLR4-MD-2 complex revealed similar interactions with key residues: F440*, S441*, and L444* in the TLR4* ectodomain and R264 in the TLR4 receptor. Although hydrophobic interactions in the MD-2 pocket were similar, **1c** exhibited strong interactions (≤3 Å) with polar residues R90 and V93 in the MD-2 that were not observed with **17a**. The conformation of **1c** with an equatorial C3-ester presumably drove the binding orientation of **1c** to be opposite of **17a**, anchoring the C4-phosphate functionality to interact with the R264 residue on the TLR4 and prompting the C10 chain of the L-seryl aglycon to be at the interface of the TLR4* ectodomain. The root-mean-square deviation (rmsd) of an overlay of **1c** and **17a** docking poses was 5.547 Å. This rmsd value, together with the different binding orientations and variable key residues plausibly involved could explain the difference in potency between **1c** and **17a**.

These docking results suggest preferential selection of ionic interactions with either TLR4* or TLR4 and the DAP's terminal lipid chain engagement of the TLR4* ectodomain provides valuable insight into agonist interactions with the human TLR4−MD-2 receptor complex and may account for the immunity profile of the DAP series.

CONCLUSIONS

We have reported the successful synthesis and evaluation of a new series of chemically stable and highly active TLR4 agonists, D-(2,3-) DAPs, in which the labile 3-ester bond on the C-3 position of the non-reducing sugar has been replaced with an axial amide and phosphate bioisosteres explored on the 4-position. The DAPs were prepared in 7 to 10 linear steps using Mitsunobu reaction conditions, granting the inversion of the 3-equatorial hydroxyl of the glucosamine to the 3-axial azide, a key functionality needed to form the essential amide bond. The DAPs displayed significantly improved chemical stability over existing synthetic lipid A mimetics. Interestingly, the subtle structural substitution of the phosphate with a sulfate group in **8b** resulted in further improvements to the chemical stability, with **8b** demonstrating remarkable aqueous thermostability at 40 °C for 12 months. To account for the high thermostability, we hypothesize that the monovalent sulfate group in **8b** reduces the rate of hydrolysis of the secondary acyl chains in the nonbuffered basic medium (2% glycerol) versus the divalent phosphate and methylene phosphonate groups. The monovalent sulfate moiety does not enhance stability in the seryl series (**17a−c**) as the secondary acyl chains are alkyl chains. The new DAPs are found to be TLR4 agonists with TLR4-specific activity toward both mouse and human TLR4. When combined with an influenza antigen, the new compounds significantly improved humoral immunity to the influenza virus. Furthermore, **17a** induced high levels of nonspecific resistance (innate immune-mediated) following intranasal administration in an influenza virus challenge. The pharmacological and toxicological properties of **17a** are currently being assessed. The preclinical profile of **17a** and further evaluation of the adjuvant activity and nonspecific resistance of the DAP series in other vaccine and infectious challenge models will be shared in further publications.

EXPERIMENTAL SECTION

Chemistry. General Experimental Section. Solvents and reagents were purchased and used without further purification. Moisture- or air-sensitive reactions were conducted under a nitrogen or argon atmosphere in oven-dried (120 °C) glassware. Solvents were removed under reduced pressure using rotary evaporators. Thin-layer chromatography (TLC) was performed on precoated EMD Millipore TLC silica gel 60 F254 glass plates with visualization by UV light (254 nm) and by staining with an ethanolic acidic vanillin solution (vanillin/water/ethanol/sulfuric acid, 0.2 g:5 mL:5 mL:1 mL). Flash chromatography purification was performed using Standard Silica Flash Cartridges on a Büchi Reveleris X2 flash chromatography system. Optical rotation values were measured using a JASCODIP-360 polarimeter at a specified temperature in the specified solvent. NMR (^{1}H, ^{1}H−^{1}H COSY, and ^{13}C) spectra were recorded on a Varian 400 or 500-MR DD2 magnetic resonance system in the noted solvent using tetramethylsilane as an internal standard. Purity for all final compounds was confirmed to be greater than 95% by RP-HPLC with UV detection using a ThermoVanquish Core HPLC with Avantor ACE 3 C8 column (50 × 3 mm, with a flow rate of 0.8 mL/min, a temperature of 60 °C, and detection at 210 nm) with a 50−100% gradient of 5 mM tetrabutylammonium hydroxide (TBAOH) water/acetonitrile to 5 mM TBAOH/acetonitrile. High-resolution mass spectra were obtained on the LC-QTOF using an ACE 3 C8 column (50 × 3.0 mm^2, with a flow rate of 0.5 mL/min, a temperature of 40 °C, and a detection at 210 nm) with a 0−100% gradient of 0.5 M ammonium carbonate/water to 0.5 M ammonium carbonate/2-propanol in an Agilent 6546 accurate-mass TOF. Compounds were formulated at 2 mg/mL in 2% glycerol.

*2-(Benzyloxycarbonylamino)ethyl 4,6-O-benzylidene-2-deoxy-2-benzyloxycarbonylamino-β-D-glucopyranoside (**2**).*[54] $[\alpha]_D^{20}$ = +17.7° ($CDCl_3$, c 0.33); ^{1}H NMR (400 MHz, $CDCl_3$): δ (ppm) 7.49−7.47 (m, 2H, H-aromatic), 7.40−7.28 (m, 13H, H-aromatic), 5.52 (s, 1H, H-benzylidene), 5.22 (br s, 2H, NH), 5.12−4.99 (m, 4H, 2 × H of CH_2 (Cbz)), 4.58 (d, $J_{1,2}$ = 8 Hz, 1H, H-1), 4.31 (dd, $J_{5,6a}$ = 5 and $J_{6b,6a}$ = 10.5 Hz, 1H, H-6a), 3.95 (br s, 1H, H of N−CH_2 (CH_2−CH_2)), 3.86−3.81 (m, 1H, H-6b), 3.75 (t, $J_{2,3} \cong J_{3,4}$ = 10 Hz, 1H, H-4), 3.67 (br s, 1H, H-

https://doi.org/10.1021/acs.jmedchem.3c00724
J. Med. Chem. 2023, 66, 13900−13917

3), 3.54 (t, $J_{1,2} \cong J_{2,3}$ = 9 Hz, 1H, H-2), 3.48−3.39 (m, 3H, H of N−CH_2 (CH_2−CH_2), H of O−CH_2 (CH_2−CH_2) and H-5), 3.31−3.23 (m, 2H; H of O−CH_2 (CH_2−CH_2) and 3-OH (exchangeable with D_2O)); ^{13}C NMR (100 MHz, $CDCl_3$ + 1 drop CD_3OD): δ (ppm) 157.2, 156.8, 136.9, 136.4, 136.2, 129.2, 128.4, 128.4, 128.2, 128.0, 128.0, 127.9, 127.9, 126.2, 101.8, 81.3, 70.9, 69.0, 68.5, 66.9, 66.6, 66.2, 58.3, 40.6; HRMS (ESI+, m/z) calcd for $C_{31}H_{34}N_2O_9$ $[M + H]^+$, 579.2343; found, 579.2329.

*2-(Benzyloxycarbonylamino)ethyl 4,6-O-benzylidene-3-O-acetate-2-deoxy-2-benzyloxycarbonylamino-β-D-glucopyranoside (**2a**).* To a stirred solution of **2** (0.050 g, 0.086 mmol) in anhydrous CH_2Cl_2 (1.0 mL) was added TEA (0.036 mL, 0.17 mmol), acetic anhydride (0.016 mL, 0.17 mmol), and a catalytic amount of DMAP. The reaction mixture was stirred at room temperature for 1 h and sequentially washed with a saturated solution of $NaHCO_3$, NH_4Cl, and H_2O. The organic layer was dried over anhydrous Na_2SO_4 and concentrated under vacuum. The resulting residue was purified with a Reveleris X2 system (Büchi) using a gradient of 10−90% ethyl acetate/heptane to provide the acetate **2a** as a white solid (13 mg, 26% yield). ^1H NMR (500 MHz, $CDCl_3$): δ (ppm) 7.44−7.42 (m, 2H, H-aromatic), 7.37−7.25 (m, 13H, H-aromatic), 5.49 (s, 1H, H-benzylidene), 5.27 (br s, 1H, NH), 5.21 (t, $J_{2,3} \cong J_{3,4}$ = 10 Hz, 1H, H-3), 5.15−5.03 (m, 4H, 2 x H of CH_2 (Cbz)), 4.97 (br s, 1H, NH), 4.41 (d, $J_{1,2}$ = 7 Hz, 1H, H-1), 4.31 (dd, $J_{5,6a}$ = 5 and $J_{6a,6b}$ = 10.5 Hz, 1H, H-6a), 3.82 (br s, 1H, H of N−CH_2 (CH_2−CH_2)), 3.78−3.72 (m, 2H, H-4, and H-6b), 3.65 (t, $J_{1,2} \cong J_{2,3}$ = 9.5 Hz, 1H, H-2), 3.57−3.55 (m, 1H, H of N−CH_2 (CH_2−CH_2)), 3.50−3.45 (m, 1H, H-5), 3.39 (br s, 1H, H of O−CH_2 (CH_2−CH_2)), 3.28 (br s, 1H, H of O−CH_2 (CH_2−CH_2)), 2.00 (s, 3H, CH_3 of 3-OAc).

*2-(Benzyloxycarbonylamino)ethyl 3-azido-4,6-O-benzylidene-2-benzyloxycarbonylamino-2,3-dideoxy-β-D-allopyranoside (**3**).* To a stirred solution of **2** (4.0 g, 6.91 mmol) in anhydrous tetrahydrofuran (THF, 100 mL) was added TEA (1.45 mL, 10.36 mmol) and triphenylphosphine (2.90 g, 11.06 mmol). The reaction mixture was cooled to 0 °C, and DIAD (2.18 mL, 10.36 mmol) and DPPA (2.38 mL, 10.36 mmol) were added. The resulting reaction mixture was gradually warmed up to room temperature and stirred for 18 h. THF was removed by evaporation, and the resulting residue was purified with a Reveleris X2 system (Büchi) using a gradient of 20−70% ethyl acetate/heptane to provide the azide **3** as a white solid (3.25 g, 79% yield). $[\alpha]_D^{20}$ = −51.5° ($CDCl_3$, c 0.33); ^1H NMR (400 MHz, $CDCl_3$): δ (ppm) 7.49−7.48 (m, 2H, H-aromatic), 7.41−7.31 (m, 13H, H-aromatic), 5.56 (s, 1H, H-benzylidene), 5.35 (d, J = 8 Hz, 1H, NH), 5.25 (br s, 1H, NH), 5.14−4.97 (m, 4H, 2 × H of CH_2 (Cbz)), 4.51 (d, J = 12 Hz, 1H, H-1), 4.36−4.30 (m, 2H, H-6a and H-3), 3.96−3.93 (m, 1H, H-6b), 3.86−3.74 (m, 4H, H-2, H-4 and 2H of N−CH_2 (CH_2−CH_2)), 3.65−3.60 (m, 1H, H-5), 3.48−3.45 (m, 1H, H of O−CH_2 (CH_2−CH_2)), 3.31−3.25 (m, 1H, H of O−CH_2 (CH_2−CH_2)); ^{13}C NMR (100 MHz, $CDCl_3$): δ (ppm) 156.6, 155.8, 136.7, 136.5, 136.0, 129.5, 129.2, 128.6, 128.5, 128.4, 128.2, 128.1, 128.0, 126.2, 125.9, 102.0, 100.2, 78.8, 78.6, 69.0, 68.8, 67.6, 67.3, 67.1, 66.8, 66.5, 64.3, 64.1, 61.4, 52.8, 52.6, 40.6; HRMS (ESI+, m/z) calcd for $C_{31}H_{33}N_5O_8$ $[M + H]^+$, 604.2407; found, 604.2385.

*2-(Benzyloxycarbonylamino)ethyl 4,6-O-benzylidene-2-benzyloxycarbonylamino-3-acetamide-2,3-dideoxy-β-D-allopyranoside (**3a**).* To a solution of **3** (2.95 g, 4.89 mmol) in anhydrous THF (100 mL) was added a solution of 0.1 N sodium hydroxide (9.8 mL, 0.98 mmol) and a solution of 1.0 M trimethylphosphine (7.8 mL, 7.82 mmol). The reaction mixture was stirred at room temperature for 18 h. THF was removed by evaporation, and the resulting residue was purified by a Reveleris X2 system (Büchi) using a gradient of 30−100% ethyl acetate/heptane then 0−10% methanol/chloroform affording the corresponding 3-amine as a white solid (2.37 g). ^1H NMR (400 MHz, $CDCl_3$): δ (ppm) 7.48−7.46 (m, 2H, H-aromatic), 7.40−7.30 (13H, H-aromatic), 5.58−5.50 (m, 2H, H-benzylidene and NH), 5.34 (br s, 1H, NH), 5.14−4.97 (m, 5H, 2x CH_2 of Cbz and 1H of 3-NH_2), 4.35 (d, $J_{1,2}$ = 8 Hz, 1H, H-1), 4.03 (dd, $J_{5,6a}$ = 4.7 and $J_{6a,6b}$ = 10.1 Hz, 1H, H-6a), 3.63−3.31 (m, 7H, 1H of 3-NH_2, H-2, H-3, H-4, 2H of N−CH_2 (CH_2−CH_2), H-6b), 3.14 (br s, 1H, H of O−CH_2 (CH_2−CH_2)), 3.00 (br s, 1H, H of O−CH_2 (CH_2−CH_2)). To a stirred solution of the 3-amine (0.030 g, 0.052 mmol) in anhydrous methylene chloride (1.0 mL) was added TEA (0.016 mL), acetic anhydride (0.010 mL, 0.10 mmol), and a catalytic amount of DMAP. The reaction mixture was stirred at room temperature for 1 h and then sequentially washed with a saturated solution of $NaHCO_3$, NH_4Cl, and H_2O. The organic layer was dried over anhydrous Na_2SO_4 and concentrated under vacuum. The resulting residue was purified by a Reveleris X2 system (Büchi) using a gradient of 30−70% ethyl acetate/heptane to provide the acetamide **3a** as a light-yellow solid (30 mg, 94% yield). ^1H NMR (500 MHz, $CDCl_3$): δ (ppm) 7.42−7.26 (m, 15H, H-aromatic), 6.14 (t, J = 8.2 Hz, 1H, NH), 5.95 (br s, 1H, NH), 5.53 (s, 1H, H-benzylidene), 5.40 (br s, 1H, NH), 5.10−5.01 (m, 4H, 2 × H of CH_2(Cbz)), 4.71 (br s, 1H, H-3) 4.61 (d, $J_{1,2}$ = 9.5 Hz, 1H, H-1), 4.33 (dd, $J_{5,6a}$ = 4.8 and $J_{6a,6b}$ = 10.6 Hz, 1H, H-6a), 3.09−3.80 (m, 2H, H of N−CH_2 (CH_2−CH_2) and H-2), 3.77−3.73 (m, 2H, H-4, and H-6b), 3.68 (m,1H, H-5), 3.59−3.55 (m, 1H, H of N−CH_2 (CH_2−CH_2)), 3.39 (br s, 1H, H of O−CH_2 (CH_2−CH_2)), 3.27 (br s, 1H, H of O−CH_2 (CH_2−CH_2)), 1.99 (s, 3H, CH_3 of 3-NHAc).

*2-(Benzyloxycarbonylamino)ethyl 4,6-O-benzylidene-2-benzyloxycarbonylamino-3-[(R)-3-decanoyloxytetradecanoylamino]-2,3-dideoxy-β-D-allopyranoside (**5**).* To a stirred solution of the 3-amine (0.48 g, 0.83 mmol), prepared following Staudinger conditions reported under **3a**, in anhydrous methylene chloride (20 mL) was added (*R*)-3-decanoyloxytetradecanoic acid **4** (398 mg, 1.0 mmol) and 1-(3-(dimethylamino)propyl)-3-ethylcarbodiimide methiodide (297 mg, 1.0 mmol). The reaction mixture was stirred at room temperature for 2 h and then quenched with a saturated $NaHCO_3$ solution (5 mL). The organic layer was separated, the aqueous layer was extracted with chloroform (2 × 5 mL), and the combined organic layers were washed with water (5 mL), dried over anhydrous Na_2SO_4, and concentrated in vacuo. The resulting residue was purified by a Reveleris X2 system (Büchi) using a gradient of 10−60% ethyl acetate/heptane to afford **5** as a colorless oil (720 mg, 76% yield over two steps). $[\alpha]_D^{20}$ = −34.3° ($CDCl_3$, c 0.33); ^1H NMR (400 MHz, $CDCl_3$ + 2drops CD_3OD): δ (ppm) 7.40−7.25 (m, 15H), 6.66 (br s, 1H, H of NH exchangeable with CD_3OD), 5.95 (br s, 1H, H of NH exchangeable with CD_3OD), 5.56 (s, 1H, H of NH exchangeable with CD_3OD), 5.54 (s, 1H), 5.08−4.97 (m, 5H), 4.82 (br s, 1H), 4.56 (d, J = 8 Hz, 1H), 4.33−4.29 (m, 1H), 3.86−3.71 (m, 4H), 3.66−3.59 (m, 2H), 3.38−3.28 (m, 2H), 2.55−2.43 (m, 2H), 2.16 (t, J = 8 Hz, 2H), 1.56−1.49 (m, 4H), 1.27−1.16 (m, 30H), 0.85 (t, J = 8 Hz, 6H); ^{13}C NMR (100 MHz, $CDCl_3$ + 2 drops CD_3OD): δ (ppm) 174.1, 171.9, 156.7, 156.5, 136.8, 136.5, 136.4, 129.0, 128.4, 128.4, 128.1, 128.0, 128.0, 125.9, 110.0, 101.2, 100.4, 71.6, 69.0, 68.8, 67.0, 66.7, 64.7, 53.7, 42.1, 40.4, 34.5, 34.1, 31.9, 31.8, 29.6, 29.5, 29.4, 29.3, 29.2, 29.0, 25.2, 24.9, 22.6, 22.6, 14.1; HRMS (ESI+, m/z) calcd for $C_{55}H_{79}N_3O_{11}$ $[M + H]^+$, 958.5793; found, 958.5761.

*2-[(R)-3-Decanoyloxytetradecanoylamino]ethyl 4,6-O-benzylidene-2,3-di-[(R)-3-decanoyloxytetradecanoylamino]-2,3-dideoxy-β-D-allopyranoside (**6**).* A solution of **5** (720 mg, 0.75 mmol) in anhydrous THF (20 mL) was treated with 10% palladium on carbon (240 mg) and a trace amount of pyridine (a couple of drops) using a Parr hydrogenator at room temperature and 50 psig of hydrogen gas H_2(g) for 24 h. The reaction mixture was filtered through Celite, the residue was washed with 50% methanol in chloroform, and the filtrate was concentrated in vacuo. The resulting oil was azeotropically dried with toluene and then dried overnight under high vacuum. A solution of the resulting oil in methylene chloride (10 mL) was added dropwise to a solution of (*R*)-3-decanoyloxytetradecanoic acid **4** (660 mg, 1.65 mmol) and 1-(3-(dimethylamino)propyl)-3-ethylcarbodiimide methiodide (490 mg, 1.65 mmol) dissolved in methylene chloride (20 mL). The reaction mixture was stirred at room temperature for 3 h and then quenched with a saturated aqueous solution of $NaHCO_3$ (10 mL). The organic layer was separated, and the aqueous layer was extracted with methylene chloride (2 × 10 mL). The combined organic layers were washed with water (10 mL), dried over anhydrous Na_2SO_4, and concentrated in vacuo. The resulting residue was purified by a Reveleris X2 system (Büchi) using a gradient elution of 20−80% ethyl acetate/heptane to afford **6** as a colorless oil (715 mg, 66% yield over two steps). $[\alpha]_D^{20}$ = −21.1° ($CDCl_3$, c 0.33); ^1H NMR (400 MHz, $CDCl_3$): δ (ppm) 7.44−7.41 (m, 2H), 7.35−7.34 (m, 3H), 7.19 (d, J = 8.4 Hz,

https://doi.org/10.1021/acs.jmedchem.3c00724
J. Med. Chem. 2023, 66, 13900−13917

1H), 6.47 (br s, 1H), 6.17 (d, J = 8 Hz, 1H), 5.58 (s, 1H), 5.21−5.14 (m, 3H), 4.66 (br s, 1H), 4.55 (d, J = 8 Hz, 1H), 4.38−4.34 (m, 1H), 4.20−4.15 (m, 1H), 3.85−3.76 (m, 3H), 3.69−3.66 (m, 1H), 3.60−3.55 (m, 1H), 3.40 (br s, 2H), 2.58−2.40 (m, 6H), 2.29−2.19 (m, 6H), 1.64−1.54 (m, 12H), 1.31−1.25 (br s, 90H), 0.88 (t, J = 6 Hz, 18H); ^{13}C NMR (100 MHz, $CDCl_3$): δ (ppm) 173.9, 173.4, 173.2, 172.5, 170.4, 169.8, 136.7, 129.1, 128.2, 125.9, 101.3, 100.4, 71.7, 71.4, 71.3, 69.1, 68.1, 65.0, 52.2, 51.2, 42.8, 41.9, 41.4, 39.1, 34.6, 34.4, 34.2, 31.9, 31.9, 29.7, 29.7, 29.6, 29.6, 29.5, 29.5, 29.4, 29.3, 29.3, 29.2, 29.2, 29.1, 25.4, 25.3, 25.1, 25.0, 22.7, 14.1; HRMS (ESI+, m/z) calcd for $C_{87}H_{155}N_3O_{13}$ [M + H]$^+$, 1451.1638; found, 1451.1588.

*2-[(R)-3-Decanoyloxytetradecanoylamino]ethyl 6-O-benzyl-2,3-di-[(R)-3-decanoyloxytetradecanoylamino]-2,3-dideoxy-β-D-allopyranoside (**7**).* To a solution of **6** (400 mg, 0.282 mmol) in anhydrous methylene chloride (20 mL) cooled to 0 °C was added sodium cyanoborohydride (42 mg, 0.655 mmol), followed by trifluoroacetic acid (0.06 mL, 0.786 mmol). The reaction mixture was gradually warmed up to room temperature and stirred for 3 h. The reaction mixture was quenched with methanol (2 mL), concentrated in vacuo, reconstituted in methylene chloride, and washed with a saturated aqueous solution of $NaHCO_3$. The organic layer was separated, and the aqueous layer was extracted with methylene chloride (2 × 10 mL). The combined organic layers were dried over anhydrous Na_2SO_4 and concentrated in vacuo. The resulting residue was purified by a Reveleris X2 system (Büchi) using a gradient of 10−95% ethyl acetate/heptane to afford **7** as a colorless oil (380 mg, 93% yield). $[\alpha]_D^{20}$ = −30.7° ($CDCl_3$, c 0.33); ^{1}H NMR (400 MHz, $CDCl_3$ + 1 drop CD_3OD): δ (ppm) 7.32−7.24 (m, 5H), 5.26−5.13 (m, 3H), 4.58 (br s, 1H), 4.50 (d, J = 4 Hz, 2H), 4.33 (br s, 1H), 4.09 (t, J = 8 Hz, 1H), 3.96 (br d, J = 12 Hz, 2H), 3.75−3.62 (m, 3H), 3.49−3.44 (m, 1H), 3.35−3.24 (m, 2H), 2.76 (dd, J = 2, and 13.2 Hz, 1H), 2.47−2.20 (m, 12H), 1.54 (br s, 12H), 1.27−1.21 (m, 90H), 0.84 (t, J = 8 Hz, 18H); ^{13}C NMR (100 MHz, $CDCl_3$ + 1 drop CD_3OD): δ (ppm) 174.9, 174.4, 173.5, 170.9, 170.5, 170.3, 137.5, 128.4, 127.8, 127.8, 100.1, 73.3, 71.9, 71.6, 71.2, 70.8, 68.0, 66.6, 43.1, 42.9, 42.2, 40.9, 39.2, 34.7, 34.5, 34.4, 34.2, 31.8, 31.8, 29.6, 29.6, 29.5, 29.5, 29.4, 29.4, 29.4, 29.3, 29.2, 29.2, 29.1, 25.4, 25.2, 25.1, 25.0, 24.9, 22.6, 14.0; HRMS (ESI+, m/z) calcd for $C_{87}H_{157}N_3O_{13}$ [M + H]$^+$, 1453.1795; found, 1453.1748.

*2-[(R)-3-Decanoyloxytetradecanoylamino]ethyl 2,3-di-[(R)-3-decanoyloxytetradecanoylamino]-2,3-dideoxy-4-O-phosphono-β-D-allopyranoside Triethylammonium Salt (**8a**).* To a solution of **7** (160 mg, 0.11 mmol) in anhydrous methylene chloride (5 mL) was added dibenzyl diisopropylphosphoramidite (0.052 mL, 0.15 mmol) and 4,5-dicyanoimidazole (18 mg, 0.15 mmol). The reaction mixture was stirred at room temperature for 2 h, cooled to 0 °C, and treated with 30% hydrogen peroxide in water (2 mL) for 30 min. The reaction mixture was quenched by addition of a saturated aqueous solution of $NaHCO_3$ (5 mL) and stirred at room temperature for another 15 min. The organic layer was separated, and the aqueous layer was extracted with methylene chloride (3 × 5 mL). The combined organic layers were washed with water (5 mL), dried over anhydrous Na_2SO_4, and concentrated in vacuo. A solution of the intermediate (168 mg, 0.098 mmol) in anhydrous THF/methanol (4:1) solvent mixture (3 mL) was treated with 10% palladium on carbon (34 mg) using a Parr hydrogenator at room temperature and 50 psig of hydrogen gas H_2(g) for 24 h. The reaction mixture was filtered through Celite, and the filtrate was concentrated under vacuum. The resulting residue was purified by a Reveleris X2 System (Büchi) using a gradient of 90:10:0.5:0.5−70:30:2:0.5 of chloroform−methanol−water−TEA, then salted with TEA to afford **8a** as a white foamy triethylammonium salt (98 mg, 62% yield over three steps). $[\alpha]_D^{20}$ = −13.1° ($CDCl_3$, c 0.33); ^{1}H NMR (500 MHz, $CDCl_3/CD_3OD$): δ (ppm) 5.22−5.17 (m, 3H), 4.55−4.50 (m, 2H), 4.38 (br s, 1H), 4.07−4.03 (m, 2H), 3.77−3.74 (m, 3H), 3.45−3.28 (m, 3H), 3.07 (br s, 8H), CH_2 of Et_3N (~1.33 equiv), 2.54−2.38 (m, 6H), 2.26−2.22 (m, 6H), 1.56 (br s, 12H), 1.31−1.22 (m, 102H, including 12H, CH_3 of Et_3N), 0.84 (t, J = 7.5 Hz, 18H); ^{13}C NMR (125.7 MHz, $CDCl_3/CD_3OD$): δ (ppm) 173.9, 173.7, 173.5, 171.4, 170.8, 170.6, 100.0, 71.5, 71.2, 67.6, 62.1, 45.8, 41.4, 40.9, 39.1, 34.5, 34.5, 34.4, 34.2, 31.9, 31.8, 29.6, 29.6, 29.6, 29.6, 29.5, 29.5, 29.4, 29.3, 29.3, 29.3, 29.2, 29.2, 29.1, 29.1, 25.2, 25.2, 25.2, 25.0, 25.0, 22.6, 22.6, 14.0, 8.4; RP-HPLC purity: 98.9%; HRMS (ESI-, m/z) calcd for $C_{80}H_{152}N_3O_{16}P$ [M − H]$^-$, 1441.0832; found, 1441.0776.

*2-[(R)-3-Decanoyloxytetradecanoylamino]ethyl 2,3-di-[(R)-3-decanoyloxytetradecanoylamino]-2,3-dideoxy-4-O-sulfoxy-β-D-allopyranoside Triethylammonium Salt (**8b**).* To a solution of compound **7** (280 mg, 0.19 mmol) in anhydrous DMF (8 mL) was added sulfur trioxide TEA complex (210 mg, 1.16 mmol). The reaction mixture was heated to 50 °C for 5 h. An additional amount of sulfur trioxide TEA complex (210 mg, 1.16 mmol) was added, and the reaction mixture was stirred at 50 °C for another 18 h. The DMF was removed by evaporation, and the resulting residue (263 mg) was dissolved in a solution of anhydrous THF/methanol (4:1) solvent mixture (8 mL) and treated with 20% palladium hydroxide on carbon (100 mg) and 120 μL of TEA using a Parr hydrogenator at room temperature and 50 psig of hydrogen gas H_2(g) for 24 h. The reaction mixture was filtered through Celite, and the filtrate was concentrated under vacuum. The resulting residue was purified by a Reveleris X2 system (Büchi) using a gradient of 100:0:0:0−90:10:0.3:0.3 of chloroform−methanol−water−TEA, then salted with TEA to afford **8b** as a white foamy triethylammonium salt (150 mg, 55% yield over three steps). $[\alpha]_D^{20}$ = −20.1° ($CDCl_3$, c 0.33); ^{1}H NMR (500 MHz, $CDCl_3/CD_3OD$): δ (ppm) 9.21 (br s, 1H), 7.03 (br s, 1H), 6.92 (d, J = 5 Hz, 1H), 6.64 (br s, 1H), 5.25−5.15 (m, 3H), 4.67−4.61 (m, 3H), 4.20 (m, 2H), 3.83−3.81 (m, 3H), 3.58 (br s, 1H), 3.44−3.40 (m, 2H), 3.18 (q, J = 8 Hz, 6H, CH_2 of Et_3N (1 equiv)), 2.58−2.42 (m, 6H), 2.30−2.26 (m, 6H), 1.59 (br s, 12H), 1.38−1.24 (m, 99H, including 9H, CH_3 of Et_3N), 0.88 (t, J = 7.5 Hz, 18H); ^{13}C NMR (100 MHz, $CDCl_3/CD_3OD$): δ (ppm) 174.3, 174.1, 174.0, 171.7, 171.5, 171.1, 100.1, 72.8, 71.5, 71.4, 71.0, 67.6, 62.3, 46.7, 41.9, 41.1, 40.8, 39.2, 34.8, 34.6, 34.5, 34.4, 32.0, 29.8, 29.7, 29.6, 29.6, 29.4, 29.4, 29.3, 29.2, 25.3, 25.2, 22.8, 14.1, 8.7; RP-HPLC purity: 99.6%; HRMS (ESI-, m/z) calcd for $C_{80}H_{151}N_3O_{16}S$ [M − H]$^-$, 1441.0737; found, 1441.0714.

*2-[(R)-3-Decanoyloxytetradecanoylamino]ethyl 2,3-di-[(R)-3-decanoyloxytetradecanoylamino]-2,3-dideoxy-4-O-methylphosphono-β-D-allopyranoside Triethylammonium Salt (**8c**).* A solution of compound **7** (100 mg, 0.065 mmol) in anhydrous THF (2 mL) was cooled to 0 °C under an inert atmosphere and treated with a solution of 1 M lithium bis(trimethylsilyl)amide in THF (0.089 mL, 0.085 mmol). The reaction mixture was stirred at 0 °C for 10 min prior to dropwise addition of a THF solution (0.5 mL) of (bis(benzyloxy)phosphoryl)-methyl trifluoromethanesulfonate (50 mg, 0.24 mmol) and continued to stir at 0 °C for 2 h. The reaction mixture was quenched with 0.1 N hydrochloride (5 drops), diluted with chloroform (5 mL), and separated, and the organic layer was washed with a saturated aqueous solution of $NaHCO_3$ (2 mL). The aqueous layer was extracted with chloroform (2 × 5 mL), and the combined organic layers were dried over anhydrous Na_2SO_4 and concentrated in vacuo. The resulting residue (43 mg, 0.025 mmol) dissolved in anhydrous THF (20 mL) was hydrogenated using an H-Cube with 10% palladium on carbon [30 mm CatCart, full H_2(g) mode at 60 °C for 1 mL/min, atmospheric pressure, and 30 mL/min H_2(g)]. The reaction mixture was concentrated in vacuo, and the resulting residue was purified by a Reveleris X2 system (Büchi) using a gradient of 90:10:0.5:0.5−70:30:2:0.5 of chloroform−methanol−water−TEA. The fractions containing purified product were combined, concentrated in vacuo, redissolved in cold 2:1 chloroform−methanol (8.6 mL), and washed with cold 0.1 N aqueous hydrochloride (3.4 mL). The lower organic layer was separated and dried over anhydrous Na_2SO_4, concentrated in vacuo, and then salted with TEA to afford **8c** as a glassy triethylammonium salt (27 mg, 27% yield over three steps). $[\alpha]_D^{20}$ = −23.1 ($CDCl_3$, c 0.33); ^{1}H NMR (500 MHz, $CDCl_3/CD_3OD$): δ (ppm) 5.20−5.16 (m, 3H), 4.57−4.52 (m, 2H), 3.98 (br s, 2H), 3.87−3.63 (m, 6H), 3.45−3.37 (m, 2H), 3.31−3.29 (m, 1H), 2.54−2.37 (m, 6H, partially under CD_3OD peak), 2.28−2.22 (m, 6H), 1.56 (br s, 12H), 1.22 (br s, 90H), 0.85 (t, J = 7.2 Hz, 18H); ^{13}C NMR (125.7 MHz, $CDCl_3/CD_3OD$): δ (ppm) 174.6, 174.3, 173.8, 171.6, 171.0, 170.8, 100.1, 75.1, 72.1, 71.5, 71.4, 67.7, 62.0, 42.1, 41.2, 39.2, 34.7, 34.7, 34.6, 34.4, 32.0, 32.0, 29.8, 29.8, 29.8, 29.7, 29.7, 29.6, 29.6, 29.5, 29.4, 29.4, 29.4, 29.3, 29.3, 29.3, 25.4, 25.4, 25.3, 25.2, 22.8, 22.8, 14.2; RP-HPLC purity: 96.2%; HRMS (ESI-, m/z) calcd for $C_{81}H_{154}N_3O_{16}P$ [M + H]$^+$, 1457.1145; found, 1457.1185.

https://doi.org/10.1021/acs.jmedchem.3c00724
J. Med. Chem. 2023, 66, 13900−13917

*N-Benzyloxycarbonyl-O-[4,6-O-benzylidene-2-benzyloxycarbonylamino-2-deoxy-β-D-glucopyranosyl]-L-serine Methyl Ester (**11**).* To a solution of compounds **9** (16.8 g, 66.3 mmol) and **10** (38 g, 73.0 mmol) in anhydrous dichloromethane (250 mL) was added boron trifluoride etherate (11.3 mL, 79.6 mmol). The reaction mixture was stirred at room temperature for 16 h and then quenched with a saturated aqueous solution of $NaHCO_3$. The organic layer was separated, washed with brine, dried over anhydrous Na_2SO_4, and concentrated by evaporation to afford the corresponding triacetate glucosamine L-serine methyl ester as a viscous oil, which was used without further purification (45.5 g, quantitative). A solution of the crude triacetate (6.44 g, 9.54 mmol) in methanol (50 mL) was treated with a 6−10% solution of magnesium methoxide in MeOH (3 mL, 4.77 mmol). The reaction mixture was stirred for 16 h at room temperature, quenched with an ice-cold solution of 1 N H_2SO_4 (10 mL), concentrated in vacuo to the aqueous layer, which was extracted with $CHCl_3$ (3 × 30 mL). The combined organic layers were washed with brine, dried over anhydrous Na_2SO_4, and concentrated in vacuo affording the corresponding crude triol as a colorless oil (2.29 g, 44% yield). A solution of the triol (4.7 g, 8.57 mmol) in acetonitrile (20 mL) was treated with benzaldehyde dimethyl acetal (2.6 mL, 17.14 mmol) and camphorsulfonic acid (1.0 g, 4.28 mmol). The reaction mixture was stirred for 16 h at room temperature and quenched with a saturated aqueous $NaHCO_3$ solution. The reaction mixture was stirred for 30 min resulting in partial precipitation of product, which was collected by filtration. The biphasic filtrate was separated and extracted twice with ethyl acetate (3 × 10 mL). The combined organic layers were dried over anhydrous Na_2SO_4 and concentrated in vacuo to provide crude product. Combined lots were purified by a Reveleris X2 system (Büchi) using a gradient of 20−50% of ethyl acetate/dichloromethane to afford **11** as a white solid (4.08 g, 75% yield). $[\alpha]_D^{20} = -30.8°$ ($CDCl_3$, c 0.37); ^{1}H NMR (400 MHz, $CDCl_3$): δ (ppm) 7.49−7.47 (m, 2H, H-aromatic), 7.38−7.26 (m, 13H, H-aromatic), 5.75 (d, J = 7,6 Hz, 1H, NH), 5.53 (s, 1H, H-benzylidene), 5.20 (br s, 1H, NH), 5.12−5.01 (m, 4H, 2 × H of CH_2 (Cbz)), 4.62 (d, $J_{1,2}$ = 8 Hz, 1H, H-1), 4.55−4.51 (m, 1H, N−CH), 4.32 (dd, $J_{5,6a}$ = 5 and $J_{6a,6b}$ = 10.6 Hz, 1H, H-6a), 4.16 (dd, $J_{5,6b}$ = 4.3 and $J_{6a,6b}$ = 10.6 Hz, 1H, H-6b)), 3.96−3.91 (m, 2H, H-2 and H-5), 3.78−3.73 (m, 4H, H-3 and CH_3 of CO_2CH_3), 3.53 (t, J = 9 Hz, 1H, H-4), 3.45−3.37 (m, 2H, 2 x H of OCH_2), 3.26 (br s, 1H, 3-OH); ^{13}C NMR (100 MHz, $CDCl_3$): δ (ppm) 170.2, 156.8, 156.2, 136.9, 136.1, 136.0, 129.3, 128.5, 128.5, 128.4, 128.3, 128.2, 128.1, 126.3, 101.9, 101.12, 81.3, 71.4, 69.2, 68.5, 67.3, 67.2, 66.2, 58.4, 53.9, 52.8; HRMS (ESI+, m/z) calcd for $C_{33}H_{36}N_2O_{11}$ $[M + H]^+$, 637.2397; found, 637.2365.

*N-Benzyloxycarbonyl-O-[3-azido-4,6-O-benzylidene-2-benzyloxycarbonylamino-2,3-dideoxy-β-D-allopyranosyl]-L-serine Methyl Ester (**12**).* To a solution of **11** (808 mg, 1.27 mmol) in anhydrous THF (35 mL) was added TEA (0.27 mL, 1.90 mmol) and triphenylphosphine (531 mg, 2.03 mmol). The reaction mixture was cooled to 0 °C, and DIAD (0.40 mL, 2.03 mmol) and DPPA (0.44 mL, 2.03 mmol) were added. The reaction mixture was gradually warmed up to room temperature and stirred for 18 h. The solvent was removed by evaporation, and the resulting residue was purified by a Reveleris X2 system (Büchi) using a gradient of 20−70% of ethyl acetate/heptane to afford azide **12** as a white foamy solid (656 mg, 78% yield). $[\alpha]_D^{20} = -64.0°$ ($CDCl_3$, c 0.4); ^{1}H NMR (400 MHz, $CDCl_3$): δ (ppm) 7.52−7.49 (m, 2H, H-aromatic), 7.41−7.33 (m, 13H, H-aromatic), 5.76 (d, J = 7.5 Hz, 1H, NH), 5.57 (s, 1H, H of benzylidene), 5.39 (d, J = 7.5 Hz, 1H, NH), 5.20−4.99 (m, 4H, 2 × H of CH_2 (Cbz)), 4.57−4.52 (m, 2H, H-1, and N−CH), 4.39−4.33 (m, 2H, H-6a, and H-3), 4.17 (dd, $J_{5,6b}$ = 4.2 Hz, and $J_{6a,6b}$ = 10.6 Hz, 1H, H-6b), 3.99−3.70 (m, 8H, H-2, H-4, H-5, CH_3 of CO_2CH_3, 2 × H of O−CH_2); ^{13}C NMR (100 MHz, $CDCl_3$): δ (ppm) 170.1, 156.2, 155.7, 136.7, 136.0, 129.3, 128.5, 128.5, 128.4, 128.2, 128.2, 128.1, 126.1, 102.0, 100.1, 78.6, 69.1, 68.8, 67.3, 67.2, 64.2, 61.4, 53.8, 52.7, 52.6; HRMS (ESI+, m/z) calcd for $C_{33}H_{35}N_5O_{10}$ $[M + H]^+$, 662.2462; found, 662.2503.

*N-[(R)-3-Decyloxytetradecanoyl]-O-[4,6-O-benzylidene-2,3-di-[(R)-3-decyloxytetradecanoylamino]-2,3-dideoxy-β-D-allopyranosyl]-L-serine Methyl Ester (**14**).* A solution of azide **12** (3.90 g, 5.89 mmol) in a solvent mixture of THF and MeOH (4:1, 32, and 8 mL, respectively) was treated with 10% palladium on carbon (780 mg) and hydrogen H_2(g) at atmospheric pressure (balloon) for 18 h. The reaction mixture was passed through a pad of Celite, concentrated in vacuo to provide the corresponding triamine as a foamy solid, and then kept under vacuum for 18 h. A solution of (*R*)-3-decanoyloxytetradecanoic acid **13** (7.17 g, 19.44 mmol) and 1-(3-(dimethylamino)-propyl)-3-ethylcarbodiimide methiodide (5.78 g, 19.44 mmol) in anhydrous methylene chloride (20 mL) was slowly added to a solution of triamine in anhydrous methylene chloride (10 mL) and cooled to 0 °C. After stirring at room temperature for 2 h, the reaction mixture was quenched with a saturated aqueous $NaHCO_3$ solution (10 mL). The organic layer was separated, and the aqueous layer was extracted with chloroform (2 × 30 mL). The combined organic layers were washed with water (10 mL), dried over anhydrous Na_2SO_4, and concentrated in vacuo. The resulting residue was purified by a Reveleris X2 (Büchi) using a gradient of 20−60% ethyl acetate/heptane to afford the triacyl product **14** as a colorless oil (5.46 g, 63% yield over two steps). $[\alpha]_D^{20} = -27.8°$ ($CDCl_3$, c 0.36); ^{1}H NMR (400 MHz, $CDCl_3$): δ (ppm) 7.44−7.31 (m, 5H), 7.22−7.16 (m, 3H), 5.55 (s, 1H), 4.77 (br s, 2H), 4.59 (d, J = 8 Hz, 1H), 4.34−4.32 (m, 1H), 4.11−4.09 (m, 2H), 3.84−3.44 (m, 15H), 2.62 (d, J = 16 Hz, 1H), 2.46−2.33 (m, 5H), 1.55−1.54 (m, 12H), 1.40−1.01 (m, 96H), 0.89−0.87 (m, 18H); ^{13}C NMR (100 MHz, $CDCl_3$): δ (ppm) 173.1, 171.8, 171.8, 170.2, 136.9, 128.9, 128.0, 126.1, 101.5, 99.9, 69.3, 69.3, 69.1, 69.0, 68.3, 65.1, 52.5, 52.0, 51.7, 49.9, 41.5, 41.2, 40.3, 34.1, 32.7, 31.9, 30.3, 30.2, 29.8, 29.7, 29.7, 29.6, 29.5, 29.3, 26.3, 26.2, 25.7, 25.4, 25.3, 22.7, 14.1; HRMS (ESI+, m/z) calcd for $C_{89}H_{163}N_3O_{12}$ $[M + H]^+$, 1467.2315; found, 1467.2314.

*N-[(R)-3-Decyloxytetradecanoyl]-O-[6-O-benzyl-2,3-di-[(R)-3-decyloxytetradecanoylamino]-2,3-dideoxy-β-D-allopyranosyl]-L-serine Methyl Ester (**15**).* A solution of **14** (480 mg, 0.23 mmol) in anhydrous methylene chloride (10 mL) cooled to 0 °C was treated with sodium cyanoborohydride (72 mg, 1.14 mmol) and trifluoroacetic acid (0.11 mL, 1.37 mmol). The reaction mixture was gradually warmed up to room temperature and stirred for 3 h. The reaction was quenched with methanol (2 mL), concentrated in vacuo, reconstituted in methylene chloride, and then washed with a saturated aqueous $NaHCO_3$ solution. The organic layer was separated, and the aqueous layer was extracted with methylene chloride (2 × 10 mL). The combined organic layers were dried over anhydrous Na_2SO_4 and concentrated in vacuo. The resulting residue was purified by a Reveleris X2 (Büchi) using a gradient of 10−95% of ethyl acetate/heptane to afford **15** as a colorless oil (410 mg, 84% yield). $[\alpha]_D^{20} = -17.0°$ ($CDCl_3$, c 0.27); ^{1}H NMR (400 MHz, $CDCl_3$): δ (ppm) 7.34−7.24 (m, 5H), 6.92 (d, J = 8 Hz, 1H), 4.79−4.76 (m, 2H), 4.56−4.54 (m, 3H), 4.14−3.93 (m, 4H), 3.79−3.58 (m, 9H), 3.52−3.73 (m, 6H), 3.06 (br s, 1H), 2.51−2.33 (m, 6H), 1.57−1.49 (m, 12H), 1.26 (br s, 96H), 0.88 (t, J = 8 Hz, 18H); ^{13}C NMR (100 MHz, $CDCl_3$): δ (ppm) 172.4, 172.2, 171.7, 170.2, 137.9, 128.7, 128.4, 128.1, 127.8, 127.6, 100.1, 70.6, 69.6, 69.3, 69.2, 69.1, 68.4, 52.6, 52.2, 50.5, 41.9, 41.1, 40.9, 34.3, 34.1, 33.7, 31.9, 30.2, 30.1, 29.7, 29.7, 29.6, 29.4, 26.2, 26.2, 25.5, 25.3, 25.3, 22.7, 14.1; HRMS (ESI+, m/z) calcd for $C_{89}H_{165}N_3O_{12}$ $[M + H]^+$, 1469.2472; found, 1469.2448.

*N-[(R)-3-Decyloxytetradecanoyl]-O-[6-O-benzyl-4-O-dibenzylphosphino-2,3-di-[(R)-3-decyloxytetradecanoylamino]-2,3-dideoxy-β-D-allopyranosyl]-L-serine Methyl Ester (**16**).* To a solution of **15** (2.16 g, 1.47 mmol) in anhydrous methylene chloride (80 mL) was added dibenzyl diisopropylphosphoramidite (0.69 mL, 2.06 mmol) and 4,5-dicyanoimidazole (243 mg, 2.06 mmol), and the reaction mixture was stirred at room temperature for 2 h. The reaction mixture was cooled to 0 °C and treated with 30% hydrogen peroxide in water (10 mL) for 30 min. The reaction mixture was quenched by addition of a saturated aqueous $NaHCO_3$ solution (30 mL) and stirred at room temperature for 15 min. The aqueous layer was extracted with methylene chloride (3 × 20 mL), and the combined organic layers were washed with water (5 mL), dried over anhydrous Na_2SO_4, and concentrated in vacuo. The resulting residue was purified by a Reveleris X2 (Büchi) using a gradient elution of 10−70% ethyl acetate/heptane to afford the corresponding benzyl-protected phosphate intermediate **16** as a colorless oil (2.35 g, 93% yield). ^{1}H NMR (400 MHz, $CDCl_3$): δ (ppm) 7.32−7.24 (m, 15 H), 7.22 (d, J = 8 Hz, 1H), 6.87 (d, J = 8 Hz,

https://doi.org/10.1021/acs.jmedchem.3c00724
J. Med. Chem. 2023, 66, 13900−13917

1H), 6.77 (d, J = 12.0 Hz, 1H), 5.01−4.95 (m, 4H), 4.78−4.73 (m, 2H), 4.66−4.62 (m, 2H), 4.52 (s, 2H), 4.32−4.16 (m, 3H), 3.72−3.57 (m, 9H), 3.52−3.34 (m, 6H), 2.51−2.38 (m, 2H), 2.26−2.17 (m, 4H), 1.52−1.23 (m, 108H), 0.88 (t, J = 6.4 Hz, 18H); ^{13}C NMR (100 MHz, $CDCl_3$): δ (ppm) 171.6, 171.4, 170.2, 137.8, 135.4, 135.3, 128.7, 128.6, 128.4, 128.0, 127.7, 127.6, 114.2, 73.1, 69.8, 69.7, 69.3, 69.2, 60.8, 52.6, 52.3, 34.3, 34.2, 34.1, 31.9, 30.2, 30.1, 30.0, 29.8, 29.7, 29.7, 29.6, 29.5, 29.4, 29.4, 26.2, 26.2, 25.3, 25.2, 22.7, 14.1; HRMS (ESI+, m/z) calcd for $C_{103}H_{178}N_3O_{15}P$ $[M + H]^+$, 1730.3107; found, 1730.3076.

*N-[(R)-3-Decyloxytetradecanoyl]-O-[2,3-di-[(R)-3-decyloxytetradecanoylamino]-2,3-dideoxy-4-O-phosphono-]-β-D-allopyranosyl]-L-serine Triethylammonium Salt (**17a**).* A solution of **16** (2.35 g, 1.36 mmol) in anhydrous THF (30 mL) was treated with 10% palladium on carbon (470 mg) under atmospheric H_2(g) at room temperature for 18 h. The reaction mixture was filtered through Celite, and the filtrate was concentrated under vacuum. The resulting residue (1.83 g, 1.26 mmol) dissolved in THF (28 mL) and cooled to 0 °C was treated with a solution of lithium hydroxide (133 mg, 1.38 mmol) in water (1.13 mL) for 1 h. The reaction mixture was neutralized with ice-cold 1 N hydrochloride bringing the pH to 3. The organic layer was separated, and the aqueous layer was saturated with sodium chloride and extracted with chloroform (3 × 5 mL). The combined organic layers were dried over anhydrous Na_2SO_4, and the solvent was concentrated in vacuo. The resulting residue was purified by a Reveleris X2 (Büchi) using a gradient of 90:10:0.5:0.5−70:30:2:0.5 of chloroform−methanol−water−TEA. The fractions containing purified product were combined, concentrated in vacuo, redissolved in chloroform (14 mL), treated with TEA (2.2 equiv), and concentrated in vacuo to afford **17a** as a white foamy solid (750 mg, 41% over two steps). $[\alpha]_D^{20}$ = +0.2° ($CDCl_3$, c 0.33); ^{1}H NMR (500 MHz, $CDCl_3/CD_3OD$): δ (ppm) 4.60−4.57 (m, 3H), 4.32−4.28 (m, 1H), 4.10−4.04 (m, 1H), 3.72−3.62 (m, 6H), 3.46−3.31 (m, 8H),3.01 (q, J = 7.5 Hz, 8H, CH_2 of Et_3N (∼1.33 equiv), 2.48−2.20 (m, 6H), 1.51−1.45 (m, 12H), 1.33−1.20 (m, 96) 0.82 (t, J = 5 Hz, 18H); ^{13}C NMR (100 MHz, $CDCl_3/CD_3OD$): δ (ppm) 172.7, 172.2, 172.1, 99.8, 76.6, 76.5, 76.3, 69.8, 69.3, 61.6, 52.4, 45.6, 41.8, 41.2, 41.0, 34.7, 34.3, 34.2, 31.8, 30.0, 29.9, 29.6, 29.6, 29.5, 29.4, 29.4, 29.2, 26.0, 25.4, 25.2, 25.2, 22.5, 13.9, 8.23; RP-HPLC purity: 99.6%; HRMS (ESI-, m/z) calcd for $C_{81}H_{158}N_3O_{15}P$ $[M - H]^-$, 1443.1352; found, 1443.1295.

*N-[(R)-3-Decyloxytetradecanoyl]-O-[2,3-di-[(R)-3-decyloxytetradecanoylamino]-2,3-dideoxy-4-O-sulfoxy-β-D-allopyranosyl]-L-serine Triethylammonium Salt (**17b**).* To a solution of compound **15** (200 mg, 0.14 mmol) in anhydrous DMF (5 mL) was added sulfur trioxide TEA complex (148 mg, 0.82 mmol). The reaction was heated to 50 °C for 5 h. An additional amount of sulfur trioxide TEA complex (148 mg, 0.82 mmol) was added, and the reaction mixture was stirred at 50 °C for another 18 h. The DMF was removed by evaporation, and the resulting residue was dissolved in a solution of anhydrous THF/MeOH (4:1) solvent mixture (8 mL) and was treated with 20% palladium hydroxide on carbon (100 mg) and 100 μL of TEA using a Parr hydrogenator at room temperature and 50 psig of hydrogen gas H_2(g) for 24 h. The reaction mixture was filtered through Celite, and the filtrate was concentrated under vacuum. The resulting residue dissolved in THF (2 mL) and cooled to 0 °C was treated with a 4 M solution of lithium hydroxide (8 mg, 0.34 mmol) in water (0.011 mL) for 1 h. The reaction mixture was neutralized with ice-cold 1 N hydrochloride bringing the pH to 3. The organic layer was separated, and the aqueous layer was saturated with sodium chloride and extracted with chloroform (3 × 5 mL). The combined organic layers were dried over anhydrous Na_2SO_4, and the solvent was concentrated in vacuo. The resulting residue was purified by a Reveleris X2 system (Büchi) using a gradient of 90:10:0.3:0.3−70:30:2:0.5 of chloroform−methanol−water−TEA, then salted with TEA to afford **17b** as a white foamy triethylammonium salt (66 mg, 39% yield over three steps). $[\alpha]_D^{20}$ = −2.6° ($CDCl_3$, c 0.33); ^{1}H NMR (500 MHz, $CDCl_3/CD_3OD$): δ (ppm) 7.62 (d, J = 5 Hz, 1H, NH partially exchanged with CD_3OD), 7.04 (d, J = 5 Hz, 1H, NH partially exchanged with CD_3OD), 4.68−4.60 (m, 3H), 4.21−4.08 (m, 3H), 3.76−3.66 (m, 6H), 3.45−3.40 (m, 6H), 3.15 (q, J = 7.5 Hz, 5H, CH_2 of Et_3N (0.83 equiv)), 2.48−2.28 (m, 6H), 1.50 (br s, 12H), 1.35−1.24 (m, 107 H, including 8H, CH_3 of Et_3N), 0.87 (t, J = 7.5 Hz, 18H); ^{13}C NMR (100 MHz, $CDCl_3/CD_3OD$): δ (ppm) 173.3, 172.3, 172.2, 172.0, 69.7, 69.3, 69.1, 62.1, 53.1, 46.1, 41.8, 41.2, 34.4, 31.9, 30.1, 30.0, 30.0, 29.7, 29.7, 29.7, 29.6,29.5, 29.5, 29.3, 26.2, 26.1, 25.5, 25.3, 22.6, 14.5, 8.5; RP-HPLC purity: 100%; HRMS (ESI-, m/z) calcd for $C_{81}H_{157}N_3O_{15}S$ $[M - H]^-$, 1443.1257; found, 1443.1251.

*N-[(R)-3-Decyloxytetradecanoyl]-O-[2,3-di-[(R)-3-decyloxytetradecanoylamino]-2,3-dideoxy-4-O-methylphosphono-β-D-allopyranosyl]-L-serine Triethylammonium Salt (**17c**).* A solution of compound **15** (150 mg, 0.102 mmol) in anhydrous THF (2 mL) was cooled to 0 °C under an inert atmosphere and treated with a solution of 1 M lithium bis(trimethylsilyl)amide in THF (0.135 mL, 0.133 mmol). The reaction mixture was stirred at 0 °C for 10 min, before dropwise addition of a THF solution (0.5 mL) of (bis(benzyloxy)phosphoryl)-methyl trifluoromethanesulfonate (90 mg, 0.173 mmol) and continued to stir for 2 h. The reaction mixture was quenched with 0.1 N hydrochloride (5 drops), diluted with chloroform (5 mL), separated, and the organic layer was washed with a saturated aqueous $NaHCO_3$ (2 mL). The aqueous layer was extracted with chloroform (2 × 5 mL), and the combined organic layer was dried over anhydrous Na_2SO_4 and concentrated in vacuo. The resulting residue (160 mg, 0.092 mmol) dissolved in anhydrous THF (20 mL) was treated with 10% palladium on carbon (48 mg) using the Parr hydrogenator at room temperature and 50 psig of hydrogen gas H_2(g) pressure for 18 h. The reaction mixture was filtered through a pad of Celite, and the filtrate was concentrated in vacuo. The resulting residue (91 mg, 0.062 mmol) was dissolved in THF (2 mL), cooled to 0 °C, and hydrolyzed with 1 N lithium hydroxide (0.26 mL, 0.26 mmol) for 1 h. The reaction mixture was neutralized with ice-cold 1 N hydrochloride bringing the pH to 5. The layers were separated, and the aqueous layer was saturated with sodium chloride and extracted with chloroform (3 × 5 mL). The combined organic layers were dried over anhydrous Na_2SO_4 and concentrated in vacuo. The resulting residue was purified by a Reveleris X2 system (Büchi) using a gradient of 0−30% of [90:10 MeOH/H_2O]/chloroform. The fractions containing purified product were combined, concentrated in vacuo, then redissolved in cold 2:1 chloroform−methanol (14 mL) and washed with cold 0.1 N aqueous hydrochloride (5.5 mL). The lower organic layer was separated, dried over anhydrous Na_2SO_4, concentrated in vacuo, and then salted with TEA to afford **17c** as a glassy solid (56 mg, 11% over three steps): ^{1}H NMR (500 MHz, $CDCl_3/CD_3OD$): δ (ppm) 4.56−4.51 (m, 2H); 4.11 (br s, 1H); 3.95 (br s, 1H); 3.81−3.53 (m, 7H); 3.35−3.29 (m, 7H partially covered by HDO); 3.02 (q, J = 7.6 Hz, 2H, CH_2 of Et_3N (∼1/3 equiv)); 2.46−2.10 (m, 5H); 1.51−1.45 (m, 12H); 1.26−1.14 (m, 99H, including the 3H of CH_3); 0.88 (t, J = 7.0 Hz, 18H); ^{13}C NMR (100 MHz, $CDCl_3/CD_3OD$): δ (ppm) 173.0, 172.4, 172.2, 107.9, 106.3, 77.5, 76.7, 70.0, 69.6, 67.7, 46.0, 41.5, 41.3, 34.7, 34.4, 32.1, 30.3, 30.2, 29.9, 29.9, 29.8, 29.7, 29.7, 29.7, 29.5, 29.4, 26.3, 25.6, 25.5, 24.0, 22.8, 14.2, 8.5; RP-HPLC purity: 96.2%; HRMS (ESI-, m/z) calcd for $C_{82}H_{160}N_3O_{15}P$ $[M - H]^-$, 1459.1665; found, 1459.1632.

Solution Stability. A RP-HPLC method was adapted as follows for the determination of percent relative purity. Compounds and controls were formulated in 2% glycerol in water targeting a 1−2 mg/mL concentration, and the resulting formulations were sonicated until particle size (measured by dynamic light scattering) was less than 200 nm and sterile filtered through a 0.22 μm PVDF filter. Pre- and post-filtration samples were quantitated by RP-HPLC. Solutions were stored at 2−8 °C and at 40 °C. At defined times aliquots were analyzed using an Avantor Ace 3 C8 column (3 mm × 50 mm) at 60 °C with a flow rate of 0.8 mL/min. The method included gradient separation with mobile phases consisting of 5 mM TBAOH in 8% acetonitrile/water (aqueous phase) and 5 mM TBAOH in acetonitrile (organic phase). Analytes were detected at 210 nm.

Biology Transgenic HEK Cell SEAP Assays. Human (h) and mouse (m) TLR4 expressing HEK-Blue 293 cells and an NF-κB-responsive SEAP reporter gene were obtained from InvivoGen (San Diego, CA). These cells were maintained in culture media of Dulbecco's modified Eagle's medium (Cytiva, Marlborough, MA), 10% heat-inactivated FBS (Hyclone, Logan, UT), 50 U/mL penicillin, 50 μg/mL streptomycin, 100 μg/mL Normocin, 2 mM L-glutamine, and 1× HEK-Blue selection. For the assay, indicated compounds were

https://doi.org/10.1021/acs.jmedchem.3c00724
J. Med. Chem. 2023, 66, 13900−13917

serially diluted in the diluent (20 mM phosphate buffer, 1.6% glycerol), and 20 μL of a 10× final concentration was applied to the bottom of a 96-well tissue culture plate. HEK cells were applied to the plates at a density of 1×10^5 cells/well and incubated for 48 h at 37 °C. Culture supernatants were analyzed for NF-κB activation using the colorimetric SEAP detection kit Quanti-Blue (InvivoGen). Values were expressed as the fold change of OD_{650} over the average vehicle-only treated samples, and EC_{50}s were calculated by a nonlinear curve fitting (four parameters) after generating dose−response curves in GraphPad Prism.

Isolation of PBMC. Peripheral blood samples were collected from healthy adult donors with approval from the Missoula Community Medical Center Institutional Review Board and informed consent from each donor. PBMCs were isolated using a Ficoll histopaque 1.077 gradient separation and cultured at 5×10^5 cells/well in 96-well tissue culture plates with RPMI-1640 media (Cytiva, Marlborough, MA), Pen/Strep/Glutamine (Hyclone, Logan, UT), and 5% heat-inactivated human serum (Rocky Mountain Biologicals, Missoula, MT).

Cell Lines. Monomac-6 cells (MM6), human macrophage cell lines, were obtained from DSMZ (Germany). RAW264.7 cells are a murine macrophage cell line obtained from ATCC (Gaithersburg, Maryland). Cells were maintained in culture media consisting of RPMI-1640 (Cytiva, Marlborough, MA), Pen/Strep/Glutamine (Hyclone, Logan, UT), 10% heat-inactivated FBS (Hyclone, Logan, UT), and antibiotics (InvivoGen, San Diego, CA).

Cytokine Analysis. Cells were stimulated for 24 h with increasing concentrations of the indicated compounds. Culture supernatants were analyzed for MIP-1β, TNFα, RANTES, and IL-1β levels using human DuoSet (R) ELISA kits (R&D Systems, Minneapolis, MN). Values were expressed as OD_{450}, and EC_{50}s were calculated by nonlinear curve fitting (four parameters) after generating dose−response curves in GraphPad Prism.

In Vivo Experiments. Animal studies were carried out in an OLAW and AAALAC-accredited facility in accordance with the University of Montana guidelines for the care and use of laboratory animals.

Influenza Vaccination Experiments. Groups of 10 female BALB/c mice (7−9 weeks of age) were vaccinated intramuscularly with 0.3 μg HA equivalent monovalent detergent-split A/Victoria/210/2009 (H3N2; monovalent detergent-split influenza vaccine) influenza vaccine with or without the indicated concentrations of TLR4 agonists in 50 μL total volume per injection (compounds and antigen were diluted as needed in 2% glycerol in water). After 14 days, blood samples were collected via submandibular bleeds for antibody analysis, and a secondary vaccination was administered. The remaining 6 mice/group were euthanized 14dp2 (14 days postsecondary injection) by terminal cardiac puncture, and the blood was used for antibody analysis.

ELISA for Anti-Influenza Antibody Quantification. Blood was collected from mice 14 days postvaccination, and serum was isolated and diluted according to the expected antibody response (between 1:10 and 1:5000). Plates were coated with 100 μL of detergent-split A/Victoria/210/2009 influenza vaccine at 1 μg/mL. Following washing (PBS plus tween 20) and blocking (SuperBlock, Scytek Laboratories), plates were incubated with diluted serum for 1 h, followed by anti-mouse IgG, IgG1, or IgG2a-HRP secondary antibody (Bethyl Laboratories) and TMB substrate (BD). Plates were read at 450 nm. Antibody titers were determined by calculating the titer of each sample at OD 0.3.

NSR Experiments. Groups (8 mice/group) of 12−14 week-old female Balb/c mice were treated with the indicated compound and doses intranasally (10 μL/nare) under anesthesia (ketamine/xylazine) for 48 h prior to intranasal (10 μL/nare, 1LD50) infection with A/HK/68 (H3N2) mouse-adapted influenza virus. Mice were observed two times daily. Weights, disease index, and body temperatures for individual mice were recorded daily. Temperatures were measured via an infrared gun on the ventral surface of the parenteral cavity. Humane euthanasia end point criteria include weight loss of greater than 30%, a temperature of less than 77 °F or two consecutive temperatures, and a temperature of <75 °F or a grading of 4 on the behavioral ethogram score.

■ ASSOCIATED CONTENT

Supporting Information

The Supporting Information is available free of charge at https://pubs.acs.org/doi/10.1021/acs.jmedchem.3c00724.

^{1}H, ^{1}H−^{1}H COSY, and ^{13}C NMR spectra, HPLC chromatograms, conformation analysis, and biological evaluation of all new compounds (PDF)

Molecular formula strings of final DAP compounds (CSV)

Molecular Docking of **1c** in huTLR4-MD-2 complex (PDB: 3FXI) (PDB)

Molecular Docking of **8a** in huTLR4-MD-2 complex (PDB)

Molecular Docking of **8b** in huTLR4-MD-2 complex (PDB)

Molecular Docking of **8c** in huTLR4-MD-2 complex (PDB)

Molecular Docking of **17a** in huTLR4-MD-2 complex (PDB)

Molecular Docking of **17b** in huTLR4-MD-2 complex (PDB)

Molecular Docking of **17c** in huTLR4-MD-2 complex (PDB)

■ AUTHOR INFORMATION

Corresponding Author

Juhienah K. Khalaf − *Inimmune Corporation, Missoula, Montana 59802, United States;* orcid.org/0000-0001-7810-5740; Phone: 406-541-5913; Email: Juhienah.k.khalaf@inimmune.com

Authors

Laura S. Bess − *Inimmune Corporation, Missoula, Montana 59802, United States*

Lois M. Walsh − *Inimmune Corporation, Missoula, Montana 59802, United States*

Janine M. Ward − *Inimmune Corporation, Missoula, Montana 59802, United States*

Craig L. Johnson − *Inimmune Corporation, Missoula, Montana 59802, United States*

Mark T. Livesay − *Inimmune Corporation, Missoula, Montana 59802, United States*

Konner J. Jackson − *Inimmune Corporation, Missoula, Montana 59802, United States*

Jay T. Evans − *Inimmune Corporation, Missoula, Montana 59802, United States*

Kendal T. Ryter − *Inimmune Corporation, Missoula, Montana 59802, United States*

Hélène G. Bazin-Lee − *Inimmune Corporation, Missoula, Montana 59802, United States*

Complete contact information is available at: https://pubs.acs.org/10.1021/acs.jmedchem.3c00724

Author Contributions

J.K.K. wrote the manuscript. All authors have given approval to their final version of the manuscript.

Funding

This work was supported in part by the National Institute of Allergy and Infectious Diseases (NIAID) SBIR phase I and II grants no. 1 R43 and AI136081 and the Montana Board of Research and Commercialization Technology (MBRCT) no. 18-51-032. Any opinions, findings, conclusions, or recommen-

dations expressed herein are those of the authors and do not necessarily reflect the views of the NIAID and the MBRCT.

Notes

The authors declare the following competing financial interest(s): All authors were employees of Inimmune at the time the work was carried out. J.K.K., K.T.R., and H.G.B.-L. are coinventors on patents covering compounds **8a-c** and **17a-c** or their triethylammonium salt.

■ ACKNOWLEDGMENTS

The authors thank Maggie Whitacre for performing the in vivo experiments described in this study, John Hoody for acquiring ^{1}H, ^{1}H−^{1}H−COSY, and ^{13}C NMR spectra, and Cherokee Sands for providing the HPLC chromatograms of final products.

■ ABBREVIATIONS

hPBMC, human peripheral blood mononuclear cell; MPLA, monophosphoryl lipid A; TLR4, toll-like receptor 4

■ REFERENCES

(1) Excler, J. L.; Saville, M.; Berkley, S.; Kim, J. H. Vaccine development for emerging infectious diseases. *Nat. Med.* **2021**, *27* (4), 591−600.

(2) Morens, D. M.; Fauci, A. S. Emerging pandemic diseases: how we got to COVID-19. *Cell* **2020**, *182* (5), 1077−1092.

(3) Bloom, D. E.; Cadarette, D. Infectious disease threats in the twenty-first century: strengthening the global response. *Front. Immunol.* **2019**, *10*, 549.

(4) Rappuoli, R.; Pizza, M.; Del Giudice, G.; De Gregorio, E. Vaccines, new opportunities for a new society. *Proc. Natl. Acad. Sci. U.S.A.* **2014**, *111* (34), 12288−12293.

(5) Pravetoni, M.; Comer, S. D. Development of vaccines to treat opioid use disorders and reduce incidence of overdose. *Neuropharmacology* **2019**, *158*, 107662.

(6) Zhang, W.; Lin, C.; Sampath, V.; Nadeau, K. Impact of allergen immunotherapy in allergic asthma. *Immunotherapy* **2018**, *10* (7), 579−593.

(7) Brisse, M.; Vrba, S. M.; Kirk, N.; Liang, Y.; Ly, H. Emerging concepts and technologies in vaccine development. *Front. Immunol.* **2020**, *11*, 583077.

(8) Sarkar, I.; Garg, R.; van Drunen Littel-van den Hurk, S. Selection of adjuvants for vaccines targeting specific pathogens. *Expert Rev. Vaccines* **2019**, *18* (5), 505−521.

(9) Reed, S. G.; Orr, M. T.; Fox, C. B. Key roles of adjuvants in modern vaccines. *Nat. Med.* **2013**, *19* (12), 1597−1608.

(10) Coffman, R. L.; Sher, A.; Seder, R. A. Vaccine adjuvants: putting innate immunity to work. *Immunity* **2010**, *33* (4), 492−503.

(11) Pulendran, B.; S Arunachalam, P.; O'Hagan, D. T. Emerging concepts in the science of vaccine adjuvants. *Nat. Rev. Drug Discovery* **2021**, *20* (6), 454−475.

(12) Nanishi, E.; Dowling, D. J.; Levy, O. Toward precision adjuvants: optimizing science and safety. *Curr. Opin. Pediatr.* **2020**, *32* (1), 125−138.

(13) Medzhitov, R. Recognition of microorganisms and activation of the immune response. *Nature* **2007**, *449* (7164), 819−826.

(14) Federico, S.; Pozzetti, L.; Papa, A.; Carullo, G.; Gemma, S.; Butini, S.; Campiani, G.; Relitti, N. Modulation of the innate immune response by targeting toll-like receptors: a perspective on their agonists and antagonists. *J. Med. Chem.* **2020**, *63* (22), 13466−13513.

(15) Kirtland, M. E.; Tsitoura, D. C.; Durham, S. R.; Shamji, M. H. Toll-like receptor agonists as adjuvants for allergen immunotherapy. *Front. Immunol.* **2020**, *11*, 599083.

(16) De Nardo, D. Toll-like receptors: activation, signalling and transcriptional modulation. *Cytokine* **2015**, *74* (2), 181−189.

(17) Visintin, A.; Latz, E.; Monks, B. G.; Espevik, T.; Golenbock, D. T. Lysines 128 and 132 enable lipopolysaccharide binding to MD-2, leading to Toll-like receptor-4 aggregation and signal transduction. *J. Biol. Chem.* **2003**, *278* (48), 48313−48320.

(18) Johnson, A. G. Molecular adjuvants and immunomodulators: new approaches to immunization. *Clin. Microbiol. Rev.* **1994**, *7* (3), 277−289.

(19) Tamai, R.; Asai, Y.; Hashimoto, M.; Fukase, K.; Kusumoto, S.; Ishida, H.; Kiso, M.; Ogawa, T. Cell activation by monosaccharide lipid A analogues utilizing Toll-like receptor 4. *Immunology* **2003**, *110* (1), 66−72.

(20) Hawkins, L. D.; Ishizaka, S. T.; McGuinness, P.; Zhang, H.; Gavin, W.; DeCosta, B.; Meng, Z.; Yang, H.; Mullarkey, M.; Young, D. W.; Yang, H.; Rossignol, D. P.; Nault, A.; Rose, J.; Przetak, M.; Chow, J. C.; Gusovsky, F. A novel class of endotoxin receptor agonists with simplified structure, toll-like receptor 4-dependent immunostimulatory action, and adjuvant activity. *J. Pharmacol. Exp. Ther.* **2002**, *300* (2), 655−661.

(21) Jiang, Z.-H.; Budzynski, W. A.; Skeels, L. N.; Krantz, M. J.; Koganty, R. R. Novel lipid A mimetics derived from pentaerythritol: synthesis and their potent agonistic activity. *Tetrahedron* **2002**, *58*, 8833−8842.

(22) Gregg, K. A.; Harberts, E.; Gardner, F. M.; Pelletier, M. R.; Cayatte, C.; Yu, L.; McCarthy, M. P.; Marshall, J. D.; Ernst, R. K. Rationally designed TLR4 ligands for vaccine adjuvant discovery. *mBio* **2017**, *8* (3), No. e00492.

(23) Johnson, D. A.; Gregory Sowell, C.; Johnson, C. L.; Livesay, M. T.; Keegan, D. S.; Rhodes, M. J.; Terry Ulrich, J.; Ward, J. R.; Cantrell, J. L.; Brookshire, V. G. Synthesis and biological evaluation of a new class of vaccine adjuvants: aminoalkyl glucosaminide 4-phosphates (AGPs). *Bioorg. Med. Chem. Lett.* **1999**, *9* (15), 2273−2278.

(24) Bazin, H. G.; Bess, L. S.; Livesay, M. T.; Ryter, K. T.; Johnson, C. L.; Arnold, J. S.; Johnson, D. A. New synthesis of glycolipid immunostimulants RC-529 and CRX-524. *Tetrahedron Lett.* **2006**, *47* (13), 2087−2092.

(25) Bazin, H. G.; Murray, T. J.; Bowen, W. S.; Mozaffarian, A.; Fling, S. P.; Bess, L. S.; Livesay, M. T.; Arnold, J. S.; Johnson, C. L.; Ryter, K. T.; Cluff, C. W.; Evans, J. T.; Johnson, D. A. The 'Ethereal' nature of TLR4 agonism and antagonism in the AGP class of lipid A mimetics. *Bioorg. Med. Chem. Lett.* **2008**, *18* (20), 5350−5354.

(26) Stover, A. G.; Da Silva Correia, J.; Evans, J. T.; Cluff, C. W.; Elliott, M. W.; Jeffery, E. W.; Johnson, D. A.; Lacy, M. J.; Baldridge, J. R.; Probst, P.; Ulevitch, R. J.; Persing, D. H.; Hershberg, R. M. Structure-activity relationship of synthetic toll-like receptor 4 agonists. *J. Biol. Chem.* **2004**, *279* (6), 4440−4449.

(27) Bowen, W. S.; Minns, L. A.; Johnson, D. A.; Mitchell, T. C.; Hutton, M. M.; Evans, J. T. Selective TRIF-dependent signaling by a synthetic toll-like receptor 4 agonist. *Sci. Signaling* **2012**, *5* (211), ra13.

(28) Khalaf, J. K.; Bowen, W. S.; Bazin, H. G.; Ryter, K. T.; Livesay, M. T.; Ward, J. R.; Evans, J. T.; Johnson, D. A. Characterization of TRIF selectivity in the AGP class of lipid A mimetics: role of secondary lipid chains. *Bioorg. Med. Chem. Lett.* **2015**, *25* (3), 547−553.

(29) Evans, J. T.; Cluff, C. W.; Johnson, D. A.; Lacy, M. J.; Persing, D. H.; Baldridge, J. R. Enhancement of antigen-specific immunity via the TLR4 ligands MPL adjuvant and Ribi.529. *Expert Rev. Vaccines* **2003**, *2*, 219.

(30) Airhart, C. L.; Rohde, H. N.; Hovde, C. J.; Bohach, G. A.; Deobald, C. F.; Lee, S. S.; Minnich, S. A. Lipid A mimetics are potent adjuvants for an intranasal pneumonic plague vaccine. *Vaccine* **2008**, *26* (44), 5554−5561.

(31) Baldridge, J. R.; McGowan, P.; Evans, J. T.; Cluff, C.; Mossman, S.; Johnson, D.; Persing, D. Taking a toll on human disease: toll-like receptor 4 agonists as vaccine adjuvants and monotherapeutic agents. *Expert Opin. Biol. Ther.* **2004**, *4* (7), 1129−1138.

(32) Maroof, A.; Yorgensen, Y. M.; Li, Y.; Evans, J. T. Intranasal vaccination promotes detrimental Th17-mediated immunity against influenza infection. *PLoS Pathog.* **2014**, *10* (1), No. e1003875.

(33) Spinner, J. L.; Oberoi, H. S.; Yorgensen, Y. M.; Poirier, D. S.; Burkhart, D. J.; Plante, M.; Evans, J. T. Methylglycol chitosan and a synthetic TLR4 agonist enhance immune responses to influenza vaccine administered sublingually. *Vaccine* **2015**, *33* (43), 5845−5853.

https://doi.org/10.1021/acs.jmedchem.3c00724
J. Med. Chem. 2023, 66, 13900−13917

(34) Baldridge, J. R.; Cluff, C. W.; Evans, J. T.; Lacy, M. J.; Stephens, J. R.; Brookshire, V. G.; Wang, R.; Ward, J. R.; Yorgensen, Y. M.; Persing, D. H.; Johnson, D. A. Immunostimulatory activity of aminoalkyl glucosaminide 4-phosphates (AGPs): induction of protective innate immune responses by RC-524 and RC-529. *J. Endotoxin Res.* **2002**, *8* (6), 453−458.
(35) Cluff, C. W.; Baldridge, J. R.; Stöver, A. G.; Evans, J. T.; Johnson, D. A.; Lacy, M. J.; Clawson, V. G.; Yorgensen, V. M.; Johnson, C. L.; Livesay, M. T.; Hershberg, R. M.; Persing, D. H. Synthetic toll-like receptor 4 agonists stimulate innate resistance to infectious challenge. *Infect. Immun.* **2005**, *73* (5), 3044−3052.
(36) Airhart, C. L.; Rohde, H. N.; Bohach, G. A.; Hovde, C. J.; Deobald, C. F.; Lee, S. S.; Minnich, S. A. Induction of innate immunity by lipid A mimetics increases survival from pneumonic plague. *Microbiology* **2008**, *154* (7), 2131−2138.
(37) Lembo, A.; Pelletier, M.; Iyer, R.; Timko, M.; Dudda, J. C.; West, T. E.; Wilson, C. B.; Hajjar, A. M.; Skerrett, S. J. Administration of a synthetic TLR4 agonist protects mice from pneumonic Tularemia. *J. Immunol.* **2008**, *180* (11), 7574−7581.
(38) Dupont, J.; Altclas, J.; Lepetic, A.; Lombardo, M.; Vázquez, V.; Salgueira, C.; Seigelchifer, M.; Arndtz, N.; Antunez, E.; von Eschen, K.; Janowicz, Z. A controlled clinical trial comparing the safety and immunogenicity of a new adjuvanted hepatitis B vaccine with a standard hepatitis B vaccine. *Vaccine* **2006**, *24* (49−50), 7167−7174.
(39) Licea-Perez, H.; Junnotula, V.; Bowen, C. L.; Fang, K.; Qian, Y.; Matheny, C. Development of an ultra-sensitive assay for the determination of an aminoalkyl glucosaminide 4-phosphate, GSK1795091, in plasma to support a first time in human study. *Anal. Methods* **2018**, *10* (25), 3074−3080.
(40) Gao, H.-X.; Bhattacharya, S.; Matheny, C. J.; Yanamandra, N.; Zhang, S.-Y.; Emerich, H.; Li, Y.; Bojczuk, P.; Shi, H.; Wang, W.; Hopson, C.; Fu, T.; Allison, J. P.; Sharma, P.; Smothers, J. F.; Srinivasan, R.; Hoos, A. Synergy of TLR4 agonist GSK1795091, an innate immune activator, with agonistic antibody against co-stimulatory immune checkpoint molecule OX40 in cancer immunotherapy. *J. Clin. Oncol.* **2018**, *36* (15_suppl), 12055.
(41) Erwin, A. L.; Munford, R. S. Deacylation of structurally diverse lipopolysaccharides by human acyloxyacyl hydrolase. *J. Biol. Chem.* **1990**, *265* (27), 16444−16449.
(42) Johnson, D. A.; Keegan, D. S.; Sowell, C. G.; Livesay, M. T.; Johnson, C. L.; Taubner, L. M.; Harris, A.; Myers, K. R.; Thompson, J. D.; Gustafson, G. L.; Rhodes, M. J.; Ulrich, J. T.; Ward, J. R.; Yorgensen, Y. M.; Cantrell, J. L.; Brookshire, V. G. 3-O-Desacyl monophosphoryl lipid A derivatives: synthesis and immunostimulant activities. *J. Med. Chem.* **1999**, *42* (22), 4640−4649.
(43) Orr, M. T.; Kramer, R. M.; Barnes, L. t.; Dowling, Q. M.; Desbien, A. L.; Beebe, E. A.; Laurance, J. D.; Fox, C. B.; Reed, S. G.; Coler, R. N.; Vedvick, T. S. Elimination of the cold-chain dependence of a nanoemulsion adjuvanted vaccine against tuberculosis by lyophilization. *J. Controlled Release* **2014**, *177*, 20−26.
(44) Huang, G.; Dai, Y. Solid-phase synthesis of allosamidin. *Synlett* **2010**, *2010* (10), 1554−1556.
(45) Di Lorenzo, F.; Duda, K. A.; Lanzetta, R.; Silipo, A.; De Castro, C.; Molinaro, A. A journey from structure to function of bacterial lipopolysaccharides. *Chem. Rev.* **2021**, *122*, 15767−15821.
(46) Que-Gewirth, N. L.; Ribeiro, A. A.; Kalb, S. R.; Cotter, R. J.; Bulach, D. M.; Adler, B.; Girons, I. S.; Werts, C.; Raetz, C. R. A Methylated Phosphate Group and Four Amide-linked Acyl Chains in Leptospira interrogans Lipid A. *J. Biol. Chem.* **2004**, *279* (24), 25420−25429.
(47) Emmadi, M.; Kulkarni, S. S. Synthesis of rare deoxy amino sugar building blocks enabled the total synthesis of a polysaccharide repeating unit analogue from the LPS of Psychrobacter cryohalolentis K5(T). *J. Org. Chem.* **2018**, *83* (23), 14323−14337.
(48) Qin, C.; Schumann, B.; Zou, X.; Pereira, C. L.; Tian, G.; Hu, J.; Seeberger, P. H.; Yin, J. Total synthesis of a densely functionalized Plesiomonas shigelloides serotype 51 aminoglycoside trisaccharide antigen. *J. Am. Chem. Soc.* **2018**, *140* (8), 3120−3127.
(49) Posakony, J. J.; Ferre-D'Amare, A. R. Glucosamine and glucosamine-6-phosphate derivatives: catalytic cofactor analogues for the glmS ribozyme. *J. Org. Chem.* **2013**, *78* (10), 4730−4743.
(50) Luo, S. Y.; Kulkarni, S. S.; Chou, C. H.; Liao, W. M.; Hung, S. C. A concise synthesis of tetrahydroxy-LCB, alpha-galactosyl ceramide, and 1,4-dideoxy-1,4-imino-L-ribitol via D-allosamines as key building blocks. *J. Org. Chem.* **2006**, *71* (3), 1226−1229.
(51) Jiang, Z. H.; Bach, M. V.; Budzynski, W. A.; Krantz, M. J.; Koganty, R. R.; Longenecker, B. M. Lipid A structures containing novel lipid moieties: synthesis and adjuvant properties. *Bioorg. Med. Chem. Lett.* **2002**, *12* (16), 2193−2196.
(52) Lewicky, J. D.; Ulanova, M.; Jiang, Z. H. Improving the immunostimulatory potency of diethanolamine-containing lipid A mimics. *Bioorg. Med. Chem.* **2013**, *21* (8), 2199−2209.
(53) Dong, H.; Pei, Z.; Ramstrom, O. Stereospecific ester activation in nitrite-mediated carbohydrate epimerization. *J. Org. Chem.* **2006**, *71* (8), 3306−3309.
(54) Bazin-Lee, H.; Ettenger, G.; Khalaf, J.; Ryter, K. T. Toll-like Receptor Ligands. U.S. Patent 11,458,151 B2, 2019.
(55) Agoston, K.; Fugedi, P. Preparation of new type of organo-catalysts having a carbohydrate scaffold. *Carbohydr. Res.* **2014**, *389*, 50−56.
(56) Cristofalo, A. E.; Nieto, P. M.; Uhrig, M. L. Synthesis of (1->3) thiodisaccharides of GlcNAc and the serendipitous formation of 2,3-dideoxy-(1->2)-thiodisaccharides through a vinyl azide intermediate. *J. Org. Chem.* **2020**, *85* (2), 306−317.
(57) Wang, Z.; Xu, Y.; Yang, B.; Tiruchinapally, G.; Sun, B.; Liu, R.; Dulaney, S.; Liu, J.; Huang, X. Preactivation-based, one-pot combinatorial synthesis of heparin-like hexasaccharides for the analysis of heparin-protein interactions. *Chemistry* **2010**, *16* (28), 8365−8375.
(58) Vacas, T.; Corzana, F.; Jimenez-Oses, G.; Gonzalez, C.; Gomez, A. M.; Bastida, A.; Revuelta, J.; Asensio, J. L. Role of aromatic rings in the molecular recognition of aminoglycoside antibiotics: implications for drug design. *J. Am. Chem. Soc.* **2010**, *132* (34), 12074−12090.
(59) Park, B. S.; Song, D. H.; Kim, H. M.; Choi, B.-S.; Lee, H.; Lee, J.-O. The structural basis of lipopolysaccharide recognition by the TLR4-MD-2 complex. *Nature* **2009**, *458* (7242), 1191−1195.
(60) Diez-Castellnou, M.; Martinez, A.; Mancin, F. Phosphate ester hydrolysis: the path from mechanistic investigation to the realization of artificial enzymes. *Adv. Phys. Org. Chem.* **2017**, *51*, 129−186.
(61) Guthrie, J. P. Hydrolysis of esters of oxy acids: pKa values for strong acids; Brønsted relationship for attack of water at methyl; free energies of hydrolysis of esters of oxy acids; and a linear relationship between free energy of hydrolysis and pKa holding over a range of 20pK units. *Can. J. Chem.* **1978**, *56* (17), 2342−2354.
(62) Thatcher, G. R. J.; Campbell, A. S. Phosphonates as mimics of phosphate biomolecules: ab initio calculations on tetrahedral ground states and pentacoordinate intermediates for phosphoryl transfer. *J. Org. Chem.* **1993**, *58* (8), 2272−2281.
(63) Muthana, S. M.; Campbell, C. T.; Gildersleeve, J. C. Modifications of glycans: biological significance and therapeutic opportunities. *ACS Chem. Biol.* **2012**, *7* (1), 31−43.
(64) Reynolds, M. A.; Hogrefe, R. I.; Jaeger, J. A.; Schwartz, D. A.; Riley, T. A.; Marvin, W. B.; Daily, W. J.; Vaghefi, M. M.; Beck, T. A.; Knowles, S. K.; Klem, R. E.; Arnold, L. J. Synthesis and thermodynamics of oligonucleotides containing chirally pure RP methylphosphonate linkages. *Nucleic Acids Res.* **1996**, *24* (22), 4584−4591.
(65) Al-Horani, R. A.; Desai, U. R. Chemical sulfation of small molecules - advances and challenges. *Tetrahedron* **2010**, *66* (16), 2907−2918.
(66) Fei, X.; Connelly, C. M.; MacDonald, R. G.; Berkowitz, D. B. A set of phosphatase-inert "molecular rulers" to probe for bivalent mannose 6-phosphate ligand-receptor interactions. *Bioorg. Med. Chem. Lett.* **2008**, *18* (10), 3085−3089.
(67) Oblak, A.; Jerala, R. The molecular mechanism of species-specific recognition of lipopolysaccharides by the MD-2/TLR4 receptor complex. *Mol. Immunol.* **2015**, *63* (2), 134−142.
(68) Coler, R. N.; Bertholet, S.; Moutaftsi, M.; Guderian, J. A.; Windish, H. P.; Baldwin, S. L.; Laughlin, E. M.; Duthie, M. S.; Fox, C.

https://doi.org/10.1021/acs.jmedchem.3c00724
J. Med. Chem. 2023, 66, 13900−13917

B.; Carter, D.; Friede, M.; Vedvick, T. S.; Reed, S. G. Development and characterization of synthetic glucopyranosyl lipid adjuvant system as a vaccine adjuvant. *PLoS One* **2011**, *6* (1), No. e16333.
(69) Heine, H.; Adanitsch, F.; Peternelj, T. T.; Haegman, M.; Kasper, C.; Ittig, S.; Beyaert, R.; Jerala, R.; Zamyatina, A. Tailored modulation of cellular pro-inflammatory responses with disaccharide lipid A mimetics. *Front. Immunol.* **2021**, *12*, 631797.
(70) Agrawal, S.; Agrawal, A.; Doughty, B.; Gerwitz, A.; Blenis, J.; Van Dyke, T.; Pulendran, B. Cutting edge: different Toll-like receptor agonists instruct dendritic cells to induce distinct Th responses via differential modulation of extracellular signal-regulated kinase-mitogen-activated protein kinase and c-Fos. *J. Immunol.* **2003**, *171* (10), 4984−4989.
(71) Tom, J. K.; Dotsey, E. Y.; Wong, H. Y.; Stutts, L.; Moore, T.; Davies, D. H.; Felgner, P. L.; Esser-Kahn, A. P. Modulation of innate immune responses via covalently linked TLR agonists. *ACS Cent. Sci.* **2015**, *1* (8), 439−448.
(72) Wheeler, A. W.; Marshall, J. S.; Ulrich, J. T. A Th1-inducing adjuvant, MPL, enhances antibody profiles in experimental animals suggesting it has the potential to improve the efficacy of allergy vaccines. *Int. Arch. Allergy Immunol.* **2001**, *126* (2), 135−139.
(73) Eberhardt, J.; Santos-Martins, D.; Tillack, A. F.; Forli, S. AutoDock Vina 1.2.0: new docking methods, expanded force field, and python bindings. *J. Chem. Inf. Model.* **2021**, *61* (8), 3891−3898.
(74) Trott, O.; Olson, A. J. AutoDock Vina: improving the speed and accuracy of docking with a new scoring function, efficient optimization, and multithreading. *J. Comput. Chem.* **2010**, *31* (2), 455−461.
(75) Valdes-Tresanco, M. S.; Valdes-Tresanco, M. E.; Valiente, P. A.; Moreno, E. AMDock: a versatile graphical tool for assisting molecular docking with Autodock Vina and Autodock4. *Biol. Direct* **2020**, *15* (1), 12.

https://doi.org/10.1021/acs.jmedchem.3c00724
J. Med. Chem. 2023, 66, 13900−13917